OPTICAL EXCISION PROGRAM

OPTICAL CLIPPERS

PSI-ER-5538-03

LEVEL II

PROBE SYSTEMS, INCORPORATED
655 NORTH PASTORIA AVENUE
SUNNYVALE, CALIFORNIA

(6) OPTICAL EXCISION PROGRAM

OPTICAL CLIPPERS

(14) PSI-ER-5538-03

(11) 15 April 1980

(9) Rept. for 1 Jul 79-31 Mar 80

ARPA Order Number: 3621
Program Code Number: 8E20
Effective Date of Contract: 28 December 1978
Contract Expiration Date: 31 August 1980
Reporting Period: 1 July 1979 through 31 March 1980
Contract Number: N00039-79-C-0141
Principal Investigator: (10) Dave Jackson, (408)732-6550

(12) 68

DARPA NAVELEX JOINT PROGRAM
Sponsored By
Defense Advanced Research Projects Agency
ARPA Order No. 3621
Sponsored and Monitored By
NAVELEX Under Contract (5) N00039-79-C-0141
JJARPA Order-3621

409007 Jm

The views and conclusions contained in this document are those of the authors and should not be interpreted as representing the official policies, either expressed or implied, of the Defense Advanced Research Projects Agency or the U.S. Government.

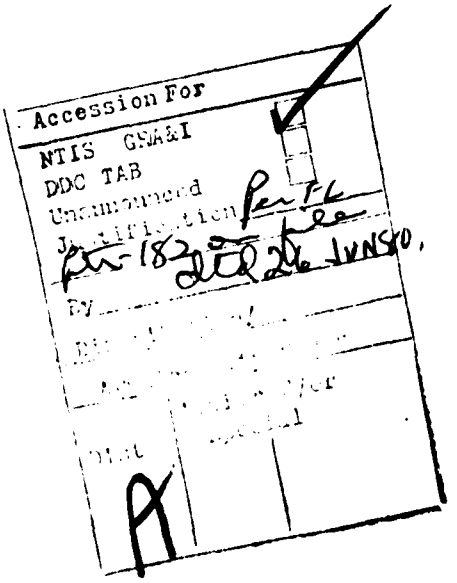

TABLE OF CONTENTS

LIST OF ILLUSTRATIONS

EXECUTIVE SUMMARY

The ability to significantly reduce the vulnerability of broadband receivers to narrowband jammer interference has been successfully demonstrated in the laboratory. The interference signal levels were attenuated by the self-adaptive frequency selective limiting properties of an optical processor invented by PROBE SYSTEMS, INC. This report describes the evaluation of optical clipper materials that, when placed in the optically-generated spectrum of a broadband RF signal, would selectively attenuate narrowband signals. The three optical clippers that were evaluated were: (1) a PROM developed by Itek Corporation and supplied by Naval Research Laboratory, (2) a selection of photodichroic crystals developed and supplied by Naval Research Laboratory, and (3) a photochromic glass purchased from Corning.

The most successful results were obtained with an optical memory developed by Itek and named the PROM. This device, when exposed to narrowband signals, affects the polarization of the transmitted light and at the same time passes those portions of broadband signals not covered by narrowband signals. By coherently detecting the transmitted light, the optical processor continuously reconstructs the broadband signals without the interference that could have degraded or even prevented further signal processing or display.

Experimental results included a test where a simulated spread spectrum radar return with a 20-MHz bandwidth was buried in noise by 4 dB. The detection probability of this signal after passing through a digital matched filter was 90% when the threshold was adjusted for less than a 10^{-6} false alarm rate. When a narrowband jamming signal was introduced at increasingly higher power levels, the detection probability would fall -- for example, at a jammer-to-signal ratio of 9 dB, the probability of detection was only 1%. When the optical signal excisor was inserted just before the digital matched filter, the probability of detection rose to almost 80%. Even at a jammer-to-signal ratio of 24 dB, the probability of detection was 50% when the excisor was used as part of the radar processor system. Spectrum analysis showed that the excisor reduced the jammer level by as much as 27 dB, almost down to the receiver noise level.

The analytical and experimental results described in this report provide clear evidence of the potential benefits that could be realized by placing an optical signal excisor in receivers used in broadband radar, communication, and intercept systems. Future investments in the optical clipper should be concentrated on the development of a PROM-like optical device that can continuously respond to the signal environment, that can be fabricated to have higher resolution, and that can be operated with considerably less support equipment. Device development work combined with PROBE's system-level analytical and experimental investigations would greatly expedite the transfer of signal excision technology to users now facing an increasingly complex electronic signal environment.

SECTION 1
INTRODUCTION

This special technical report describes the results of a task conducted by PROBE SYSTEMS as part of a DARPA/NAVELEX Joint Program for Optical Excision. The purpose of this task was to experimentally evaluate the feasibility of using optical addressed spatial light modulators to adaptively excise narrowband signals from spread spectrum signals. This work resulted in the successful demonstration of an optical excisor with an Itek PROM used in the front end of a simulated spread spectrum radar operated in the presence of a narrowband jammer. The attenuation effects of the PROM against the jammer reduced the jammer level and improved the probability of detection from 1% to 80% and permitted 50% detection probability even when the jammer was 24 dB stronger than the signal.

Optical excision is a signal processing technique for eliminating narrowband RF interference signals and has many potential applications in the areas of broadband communications, radar, and intercept systems. This technique uses an acousto-optical Bragg cell and a continuous laser to spatially form the signal spectrum of an electrical input. By blocking strong narrowband interference signals in the optically-generated signal spectrum and by coherently detecting the remainder of the spectrum, an interference-free electronic broadband signal is obtained as the output of the processor. The successful development of optical excisor technology will permit the exploration of a whole family of optical coherent processors that, in real-time, will allow access to the spectrum of a broadband signal.

Considering all of the candidate clippers for use in the coherent processor, the PROM offers many advantages. However, this device has been developed to serve as an optical memory, e.g., an electronic transparency. What is really needed in the excisor is a self-adaptive transparency that continuously responds to the incident signal spectrum. This mode of operation should also greatly simplify the support electronics and permit the development of a rack-mounted excisor.

SECTION 2
PROM DESCRIPTION

The Itek PROM is an optical device which is intended to be used as a two-dimensional, optical image storage medium. In normal use, the PROM is electronically cycled between an optical record and an optical readout stage so that the PROM acts like a real-time optical transparency. During the record stage, the PROM is "exposed" to an optical intensity image consisting of blue light such that this image is spatially stored in the PROM. During the readout stage, the PROM is illuminated with a red optical beam such that the stored image spatially modulates the optical transmittance of the red beam. Thus the net red image obtained is the product of the incident red beam times a stored image modulation function.

The physical construction of the PROM is shown in Figure 2-1. The key element of the PROM is an electro-optic, photoconductive crystal of $Bi_{12}SiO_{20}$. For the Itek PROM, this crystal is 800 μm thick and 1 inch in diameter. The crystal is sandwiched between insulating layers of parylene and transparent electrodes such that the PROM acts as a simple capacitor when no optical illumination is present. If the PROM is erased of all previous images and a voltage is placed across the transparent electrodes, an electric field will appear across the $Bi_{12}SiO_{20}$ crystal. Then if one illuminates a particular position of the PROM with a blue optical beam, the photoconductivity of the crystal causes electronic charges to be locally generated at that position. Due to the electric field across the crystal, these charges migrate to parylene-crystal interface so that the voltage drop across the crystal is decreased while the voltage drop across the parylene layers is increased. With enough optical illumination, the voltage across the crystal is reduced to zero. Since the charge migration is spatially dependent on the optical illumination of the blue beam, one can spatially control the voltage drop across the crystal of $Bi_{12}SiO_{20}$ with the blue beam.

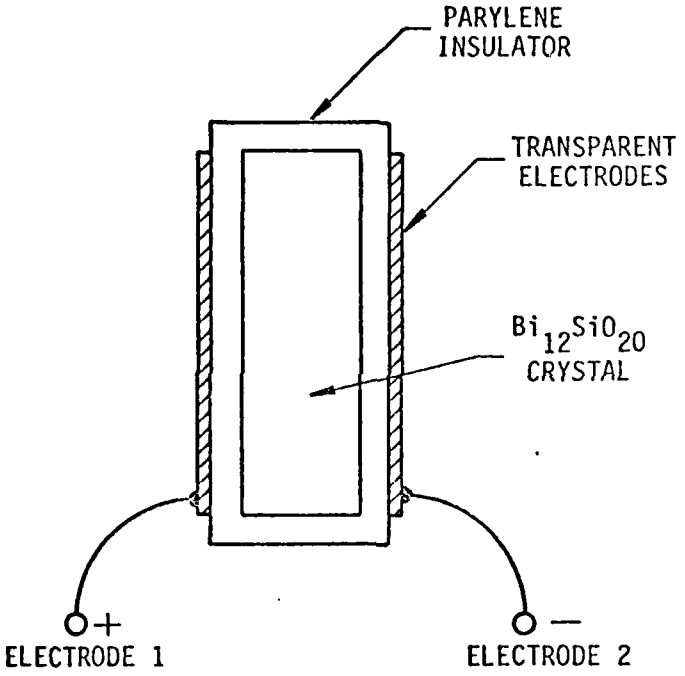

PSI-80062

FIGURE 2-1 PROM CONSTRUCTION

2. Continued

The photoconductivity of the crystal is most sensitive to optical illumination in the blue portion of the optical spectrum. For a given optical exposure of E, the voltage across the crystal will decay exponentially by the factor $\exp(-E/E_0)$ due to the photoconductivity. The quantity E_0 is the 1/e decay exposure and is a function of optical wavelength. For an optical wavelength of 4880 $\mathring{A}$ corresponding the blue line of an argon laser, $E_0 = 40$ ergs/cm^2. For an optical wavelength of 6328 $\mathring{A}$ corresponding to the red line at a helium-neon laser, $E_0 \cong 10^4$ergs/cm^2. Thus for equal intensity illumination of the $Bi_{12}SiO_{20}$ crystal with these optical wavelengths, the blue illumination will cause the voltage across the crystal to decay 250 times as fast as the red illumination.

In the readout mode, the electro-optic properties of the $Bi_{12}SiO_{20}$ crystal are utilized to modulate the polarization of a red optical readout beam. This polarization modulation is then converted to an optical intensity modulation using a polarizer. For the particular PROM utilized, the transmission mode for polarization modulation was most optically efficient. In this mode, an incident red optical beam with linear polarization is transmitted through the PROM. With no voltage across the crystal, the transmitted red beam will undergo a constant polarization rotation of roughly 18^o due to the optical activity of the crystal. Thus the exit red beam with no voltage across the crystal is linearly polarized. With a voltage across the crystal and the crystal properly oriented, the electro-optical effect will act to change the exit polarization. To convert this polarization change to an optical intensity modulation, one typically orients the exit polarizer such that with no voltage across the crystal, the polarizer blocks the exit light. Then with a voltage V across the crystal, the effective optical intensity modulation T is given by:

$$T = T_0 \sin^2\left(\frac{\pi V}{2V_H}\right) \quad . \tag{1}$$

For the PROM utilized, $V_H = 3900$ volts and is termed the half-wave voltage.

2. Continued

With the foregoing information, one can now consider the complete PROM record/readout cycle. The first step of the record stage is to erase all the previous stored image patterns in the PROM using a spatially uniform flash of blue light obtained from a flashlamp. This blue light flash makes the $Bi_{12}SiO_{20}$ crystal uniformly photoconductive so that a uniform spatial charge distribution across the device is developed. The second part of the record stage is to place a voltage V_0 across the PROM and illuminate the PROM with the desired blue light image for a time duration Δt. With a blue light image intensity distribution given by $I(x,y)$, this record procedure will produce a spatial voltage distribution across the $Bi_{12}SiO_{20}$ crystal given by:

$$V(x,y) = V_0 \exp\left[-I_B(x,y)\,\Delta t/E_{OB}\right] \quad . \tag{2}$$

In this expression, E_{OB} is the 1/e decay exposure for the blue image write beam. This completes the record stage. The optical readout stage is performed by illuminating the PROM with a red optical beam whose optical intensity distribution can be described by $I_R(x,y)$. The net effective red beam intensity I_{Rout} transmitted through the PROM-exit-polarizer combination is then given by:

$$I_{Rout} = I_R(x,y)\,T(x,y) \quad . \tag{3}$$

Since $T(x,y)$ can be obtained by combining Equations 1 and 2, the expanded version of Equation 3 takes the form:

$$I_{Rout} = I_R(x,y)\,\sin^2\left\{\frac{\pi}{2}\,\frac{V_0}{V_H}\,\exp\left[-I_B(x,y)\,\Delta t/E_{OB}\right]\right\} \quad . \tag{4}$$

2. Continued

Typically the voltage V_0 is set approximately equal to V_H to allow a maximum on-off contrast ratio. One can see from equation 4 that if the blue write beam has a high intensity at a particular position (x_0,y_0), then the red beam will be highly attenuated at that position.

Actually, Equation 4 is an approximation in that it does not include the effect of the red read beam causing photoconductivity in the crystal and writing an image of itself. Thus as time progresses, the exit red beam $I_{Rout}(x,y)$ is gradually attenuated. This attenuation is most rapid at the portions of input red beam that are most intense. To account for this effect, Equation 4 can be modified to:

$$I_{Rout} = I_R(x,y) \sin^2\left[\frac{\pi}{2}\frac{V_0}{V_H} \exp(-\alpha)\right] \tag{5A}$$

$$\alpha \triangleq I_B(x,y)\,\Delta t/E_{0B} + I_R(x,y)(t-t_0)/E_{0R} \tag{5B}$$

$$,t \geq t_0 \quad .$$

In Equation 5B, the quantity Δt represents the exposure time of the blue beam as before while the quantity $t-t_0$ represents the exposure time of the red beam which starts at the beginning of the read stage at time t_0. The quantity E_{0R} represents the 1/e decay exposure level for the red beam. Since $E_{0R} \cong 250\ E_{0B}$, the red beam exposure creating self-attenuation of the red readout beam is usually not significant unless the red exposure $I_R(t-t_0)$ is approximately 250 times greater than the blue exposure $I_B\ \Delta t$.

2. Continued

For PROBE's application of employing the PROM as an optical clipper, the blue write beam has an optical intensity distribution which is approximately (if one ignores the red reference beam intensity) proportional to the red readout beam intensity:

$$I_B(x,y) = K\, I_R(x,y) \tag{6}$$

In this equation, K is a constant of proportionality. Plugging Equation 6 into Equations 5A and B, one has for the red readout beam intensity I_{Rout} in the optical clipper mode:

$$I_{Rout}(x,y) = I_R(x,y)\, \sin^2 \left\{ \frac{\pi}{2} \frac{V_0}{V_H} \exp\left(-I_R(x,y)/\hat{I}\right) \right\} \tag{7A}$$

$$\frac{1}{\hat{I}} \triangleq \frac{K\Delta t}{E_{OB}} + \frac{t-t_0}{E_{OR}} \quad , t \geq t_0 \tag{7B}$$

One can plot I_{Rout} versus I_R as is done in Figure 2-2 with logarithmic coordinate scales and with $V_0 = V_H$. One can see that for a fixed $\hat{I}$, I_{Rout} is linearly related to I_R for I_R somewhat less than $\hat{I}$, while for I_R somewhat greater than $\hat{I}$, I_{Rout} decreases very rapidly. The maximum value of $I_{Rout}/\hat{I}$ is 0.347 and occurs at $I_R/\hat{I} = .65$. Thus it is convenient to label $\hat{I}$ as the optical clipping threshold. Note that for longer exposure times on either the blue or red beams, the clipping threshold $\hat{I}$ decreases.

The preceding discussion of the PROM has ignored a number of possible alternatives for modes of operation. For example, one has the option of adding a spatially uniform baseline subtraction voltage to the spatial voltage distribution described in Equation 2. Also, one can consider other orientations of the exit

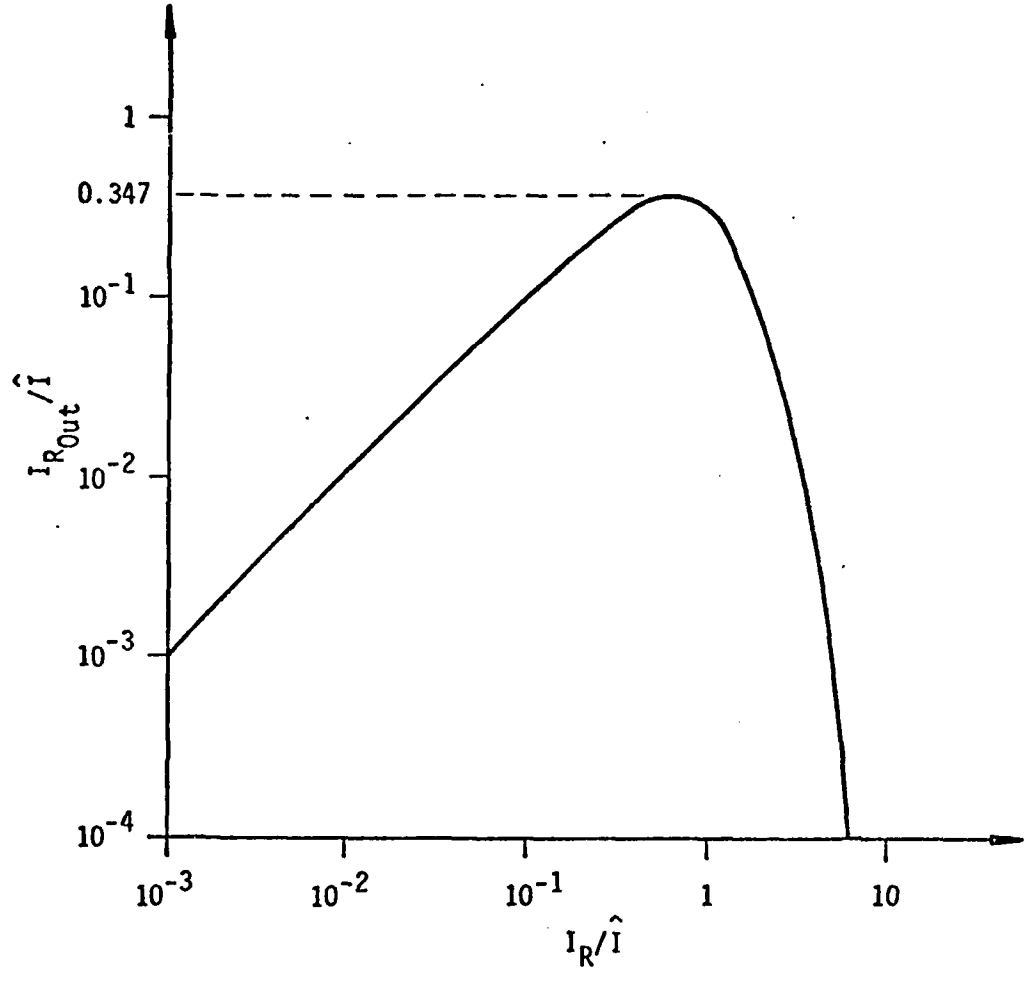

FIGURE 2-2 PLOT OF $I_{R_{Out}} = I_R \sin^2\left[\frac{\pi}{2} \exp(-I_R/\hat{I})\right]$

2. Continued

polarizer. These options can produce some interesting effects for the optical clipper application, but have the problem of not having a large attenuation for very high exposures with the write light. For this reason, these options were avoided. Also, it should be apparent from the previous discussion that it is not necessary to use any write illumination on the PROM to utilize it as an optical clipper since the read beam acts to expose the PROM and causes self clippling. This mode of operation where the PROM is cycled with no write light will produce a clipping threshold $\hat{I}$ which decreases with time from the start of the read stage at $t = t_0$:

$$\hat{I} = \frac{E_0}{t-t_0} \qquad t \geq t \ . \qquad (8)$$

The value of E_o is a function of the read light optical wavelength as before, but for this mode, the read light is not necessarily red. Plugging Equation 8 into Equation 7A, one has for the exit readout beam optical intensity I_{out} as a function of the input read beam intensity I_{in} with no write light:

$$I_{out}(x,y) = I_{in}(x,y) \sin^2 \left\{ \frac{\pi}{2} \frac{V_0}{V_H} \exp \left[-I_{in}(x,y)(t-t_0)/E_0 \right] \right\} \qquad (9)$$

The basic properties of Equation 9 are similar to those of Equation 7A except that there is always a time delay from the start of the read cycle before $\hat{I}$ becomes small enough to create optical clipping. Once should note that the exponential time delay rate in Equation 9 is proportional to the input read beam intensity I_{in}. Thus strong optical signals are attenuated more rapidly than weak optical signals for the mode of operation where no write illumination is used.

SECTION 3
OPTICAL TEST LAYOUT

The optical test layout for obtaining data in the PROM experiments is shown in Figure 3-1. This layout utilizes two separate lasers to produce the red (Hughes 5 mW HeNe laser at 6328 A) and blue (Spectra-Physica 2 mW Argon laser at 4880 A) light. One can think of the optical layout as consisting of separate red and blue optical systems which share some optical components. The red system consists of a PROBE SYSTEMS' coherent-detection, acousto-optic system using a Mach-Zehnder interferometer. The red system generates a signal beam in one path of the interferometer by passing the red light through beam expansion/ collimation optics, an acousto-optic modulator, and a Fourier transform lens.

A red reference beam is generated in the other path of the interferometer and combined with the red signal beam via a beam splitter. The combined red signal and reference beams are then passed through the Itek PROM, which is located in the Fourier transform plane of the acousto-optic modulator. This combined red beam acts as the optical readout beam for the PROM and is guaranteed to be linearly polarized by the use of a polarizer before the PROM. After passing through the PROM, the red readout beam is passed through a crossed polarizer and focused onto a photodetector to produce the coherent RF output.

All of the red light passing through the PROM is incident on the photodetector surface so that any phase perturbations produced by the PROM have no effect on the signal output. If one removed the PROM and the crossed polarizer, the red system would be the same as a conventional coherent-detection, acousto-optic system with image plane detection.

As in most other experiments, the photodetector used was the Varian VPM 152-D, which has a bandwidth of 2 GHz. The acousto-optic modulator used was the Anderson Laboratories BD-125, which has a bandwidth of 25 MHz centered at 40 MHz and a time-bandwidth product of 125 for rectangular window illumination. For the PROM experiments, the illumination was closer to Gaussian. The details of the acousto-optic cell illumination and the Fourier transform spot size are further discussed in the experimental data section.

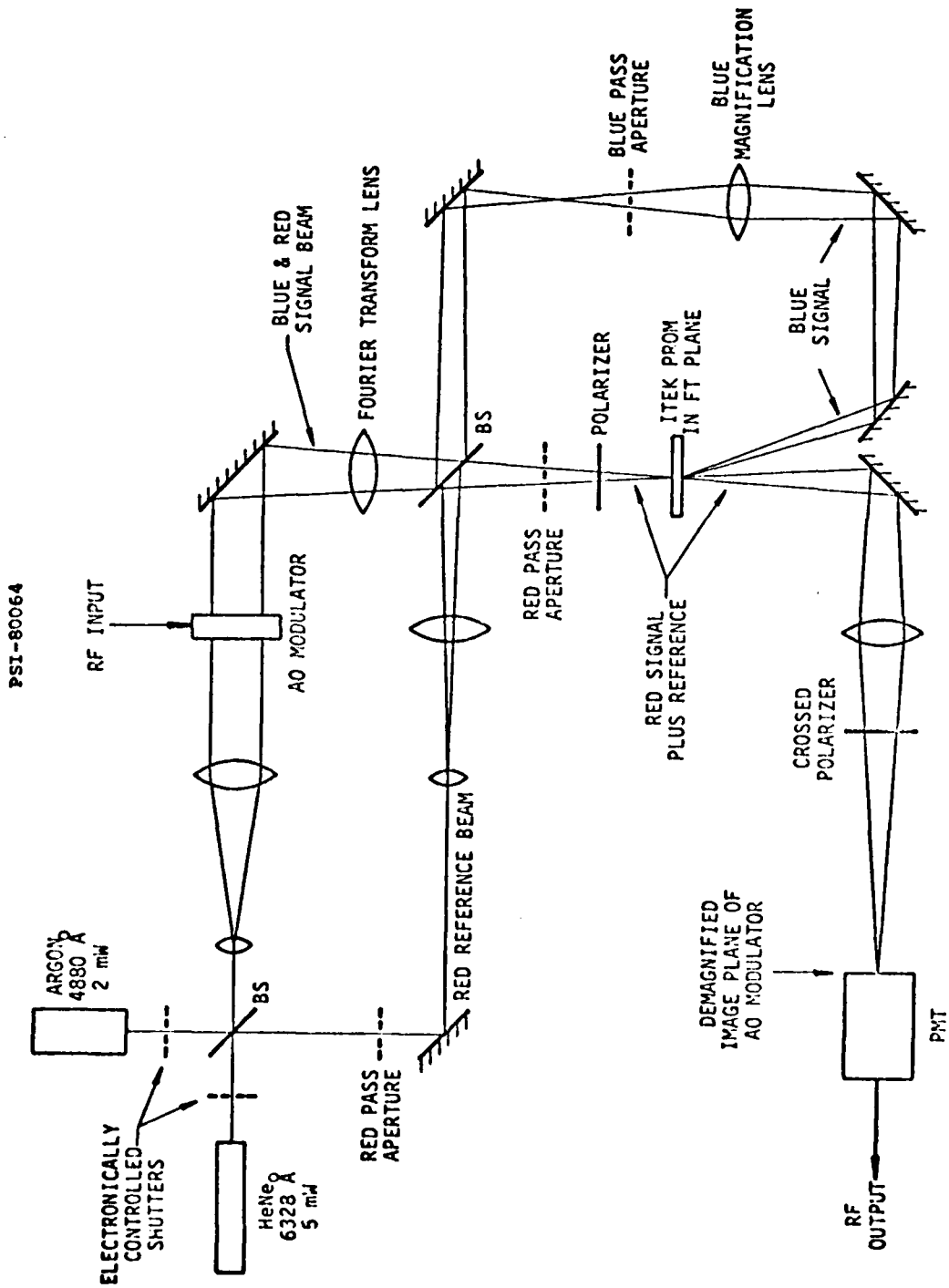

FIGURE 3-1 OPTICAL LAYOUT FOR THE PROM EXPERIMENTS

3. Continued

The blue optical system is used to obtain an image of the RF input signal spectrum which can then be used to write on the PROM during the write stage of the PROM cycle. To do this, the blue beam from the argon laser bounces off the beam splitter and passes through the beam-expansion/collimation optics, the acousto-optic modulator, and the Fourier transform lens in a manner similar to the red signal beam. The blue signal beam then bounces off the second beam splitter and passes through an optical path which acts to magnify and image the blue Fourier transform plane onto the reverse side of the PROM. This magnification is necessary to match the blue spatial Fourier transform to the red signal beam Fourier transform because the size of the spatial Fourier transform is proportional to wavelength. Thus the blue Fourier transform must be magnified by the factor 6328/4880 = 1.30.

In order to have the blue Fourier transform match spatially with the red Fourier transform, very fine positioning to within ±25 micrometers for the blue beam is required. This positioning was obtained by micrometer screw adjustments which controlled the tilt of the blue beam mirrors. One should note that the blue optical system is separated from the red by use of "redpass" and bluepass" apertures. This is possible because the red and blue beams are not exactly collinear and are tilted with respect to each other in a direction out of the page in Figure 3-1. The tilt between the red and blue beams is such that they coincide when passing through the acousto-optic modulator but are separate at significant distances from the acousto-optic modulator.

One should also note in Figure 2-2 that the blue reference beam is blocked so that only the blue signal beam is used for writing on the PROM. Finally, one should note that electronically-controlled shutters are used to alternately select the blue and red lasers for the record and readout stages of the PROM cycle.

SECTION 4
EXPERIMENTAL DATA

A considerable number of experimental measurements were performed to examine the capabilities of the PROM as an optical clipper. One should keep in mind when examining this data that the PROM is a storage device so that all data written on the PROM remains stored until the next erase/record stage of the PROM cycle. Thus the Itek PROM is not a true real-time device in the sense that it must be continually cycled through the erase/record and read cycles.

4.1 OPTICAL QUALITY OF THE PROM

One of the first characteristics of the PROM which was examined before procedding with the optical clipping experiments was its optical quality. By passing the red reference beam through the PROM with no polarizers and then magnifying and examining the exit red beam, one could see the beam distortion caused by the PROM. While the incident red reference beam was a smooth looking line at roughly 1 millimeter in width and 20 millimeters in length, the exit red beam was jagged and had a number of gaps in it corresponding to dirt specs on the PROM. After considerable positioning, a location on the PROM was found which had a mild amount of distortion. This location was used for subsequent experiments. Unfortunately, the exposed PROM surfaces could not be cleaned because they were comprised of the unprotected and soluble transparent electrodes.

To examine the effects of the PROM's optical distortion on the coherent-detection output, the output of the optical system was examined for an RF pulse input. The input RF pulse is shown in Figure 4-1A and consists of approximately nine cycles of a 40-MHz sine wave with a 14.5 volt peak-to-peak amplitude. This signal level represents roughly a 40% diffraction efficiency for the acousto-optic modulator. The coherently detected output pulse with the PROM physically *removed* from the optical system of Figure 3-1 is shown in Figure 4-1B. Notice that even without the PROM there is significant distortion in the form of after

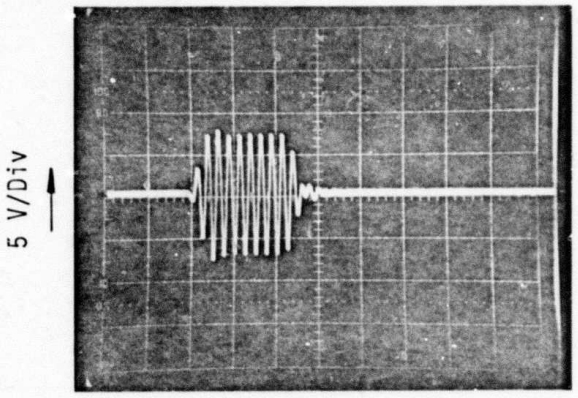

A. INPUT RF PULSE AT 40 MHz CENTER FREQUENCY

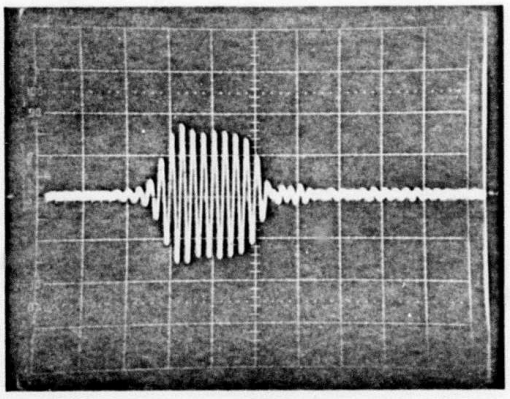

B. COHERENT DETECTION OUTPUT PULSE WITH NO PROM

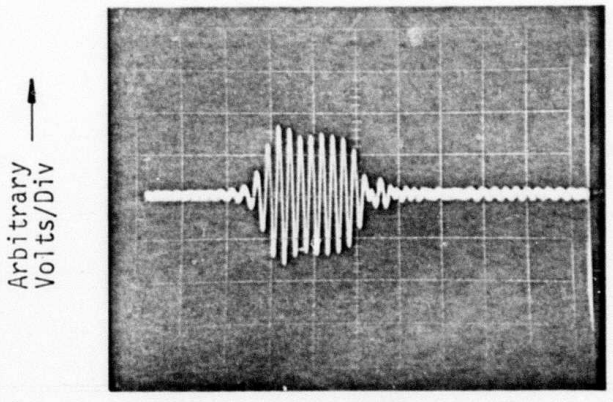

C. COHERENT DETECTION OUTPUT PULSE WITH PROM IN FOURIER TRANSFORM PLANE

FIGURE 4-1 RF PULSE INPUT AND OUTPUT

4.1 Continued

pulse ringing. This ringing is believed to be due to an optical reflection created by a non-antireflection coated cylindrical lens for the beam expanding optics. This optical reflection is further examined in Section 4.2, which discusses the acousto-optic modulator illumination. The PROM was then inserted into the optical system of Figure 2-2 with no voltage across the PROM and the exit polarizer not crossed. In this mode, the PROM should have no spatial modulation and not affect the coherent detection output. The coherently detected output pulse with the PROM in this mode is shown in Figure 4-1C. Comparing Figures 4-1B and 4-1C, one sees that the PROM does not significantly affect the coherently detected output despite its mild beam distortion. There is, however, a small amount of distortion created which is evident from the difference in after pulse ringing between Figures 4-1B and 4-1C.

One final optical characteristic of the PROM involves its optical attenuation in the transmission mode. With no exit polarizer, the PROM attenuates the transmitted beam intensity to approximately 50% of the input beam intensity. This high amount of attenuation is believed to be caused by the optical index of refraction mismatches between the adjacent layers of the PROM.

4.2 THE ACOUSTO-OPTIC MODULATOR ILLUMINATION AND THE FOURIER TRANSFORM PLANE INTENSITIES

To avoid the sidelobes in the spatial Fourier transform plane which are associated with uniform spatial illumination of the acousto-optic modulator, the illumination of the acousto-optic modulator aperture was made nearly Gaussian in the direction of the sound propagation. The illumination immediately after the acousto-optic modulator aperture was experimentally measured using a narrow razor blade slit attached to the front of an NRC photodetector head which was in turn mounted on a linear translation stage. This measured illumination intensity is plotted in Figure 4-2. The total width of the acousto-optic modulator aperture is 20.6 millimeters so that one can see from Figure 4-2 that nearly the entire

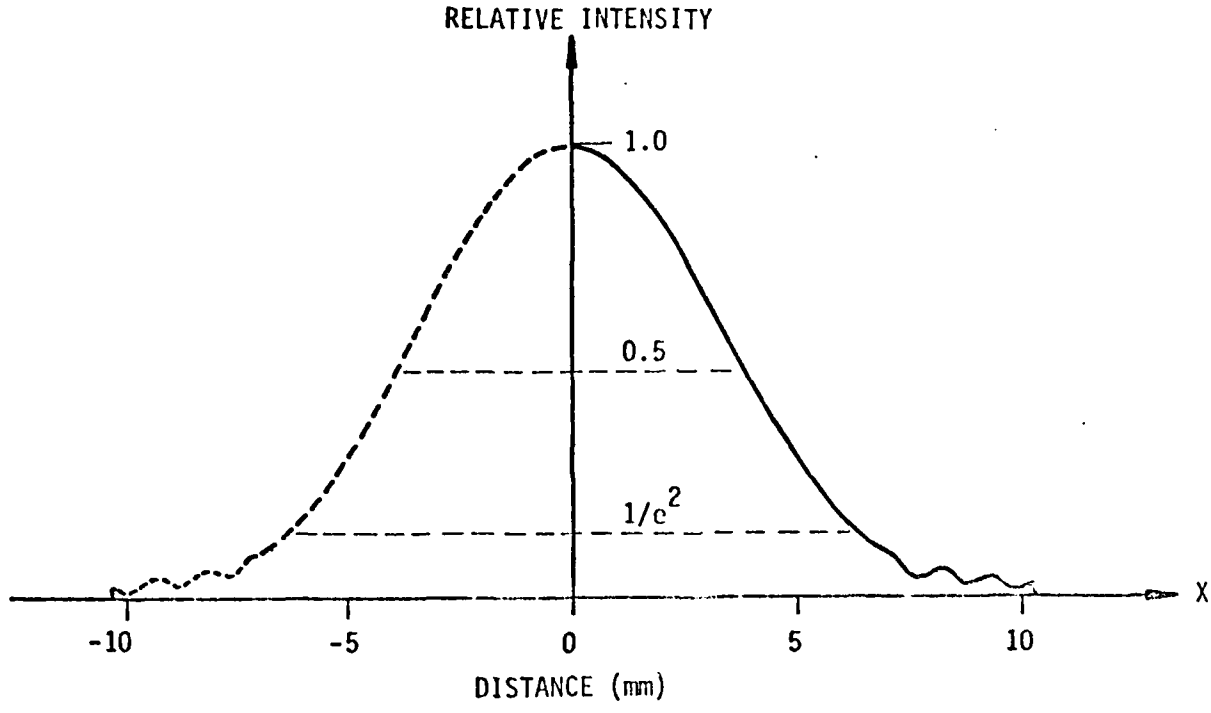

PSI-80065

FIGURE 4-2 ACOUSTO-OPTIC APERTURE ILLUMINATION

4.2 Continued

signal beam was contained within this aperture. Actual data was taken only for $x \geq 0$ due to the limits of the translation stage movement. The data shown as a dotted line for $x < 0$ is actually a reflection of the data for positive values of x. This is a reasonable approximation due to the symmetry of the signal beam illumination. Note that there is some "ripple" in the illumination intensity near the edges of the acousto-optic modulator aperture. This ripple appears to be created by a double reflection of the optical signal beam off the surfaces of the non-antireflection coated cylindrical lens used for the signal beam expansion. This reflection cannot be eliminated by tilting the lens, so that the only cure appears to be to use anti-reflection coated cylindrical lenses for the optical beam expansion. This approach will be tested at a future date on another contract, but is not reported here. As previously mentioned, this double reflection is the suggested cause of the after pulse ringing of Figures 4-1B and 4-1C.

By examining Figure 4-2 one can calculate the effective time-bandwidth product of the acousto-optic modulator for the acousto-optic window illumination used. The half-power intensity width of the illumination is seen to be approximately 7.5 millimters while the $1/e^2$ intensity width is approximately 13 millimeters. To calculate the effective time-bandwidth product, one should use optical amplitude because the diffracted signal beam amplitude is proportional to the input electrical signal amplitude. Since the time-bandwidth product of the acousto-optic modulator with full aperture, uniform illumination is 125 and the full aperture width is 20.6 millimeters, the 3 dB amplitude time-bandwidth product is given by $(7.5/20.6) \times 125 \cong 46$ while the 1/e amplitude time-bandwidth product is given by $(13/20.6) \times 125 \cong 79$.

It is useful to estimate the optical intensity distribution on the PROM surface. The PROM is located in the spatial Fourier transform plane at the acousto-optic modulator so that a single frequency input signal to the modulator will create an optical signal beam amplitude distribution on the PROM which is

4.2 Continued

the spatial Fourier transform of the acousto-optic modulator optical amplitude illumination. From this one can calculate the intensity distribution $I_{SR}(x,y)$ at the red signal beam at the PROM surface. Assuming that the illumination of Figure 4-2 is approximately Gaussian with a 1/e amplitude width of 13 millimeters, and taking into account the optical wavelength (6328 Å) and the focal length of the Fourier transform lens (48"), one has for the red signal beam intensity:

$$I_{SR}(x,y) \cong \left(\frac{DE}{100\%}\right) K_R \; e^{-\left(\frac{y}{0.1}\right)^2} \; e^{-\left(\frac{x-x_o}{0.0027}\right)^2} \quad . \tag{10}$$

In this equation DE represents the first order diffraction efficiency, K_R is a constant of proportionality, and distances x and y are in centimeters. The variable x_o is proportional to frequency and represents the center location of the diffracted signal beam spot. The 1/e optical intensity width in the y direction at 0.2 centimeters is obtained from a rough visual estimate while the 1/e intensity width in the x direction at .0054 centimeters is calculated* from a spatial Fourier transform of the measured illumination of Figure 4-2. To obtain the constant K_r; the total first order diffraction optical power hitting the PROM was measured as being 57μW at a diffraction efficiency of 12%. Integrating equation 10 over x and y and equating the result to 57μW, one can solve for K_R and obtain:

$$I_{SR}(x,y) \cong \left(\frac{DE}{100\%}\right)(.56)e^{-\left(\frac{y}{0.1}\right)^2} e^{-\left(\frac{x-x_o}{0.0027}\right)^2} \quad \frac{\text{Watts}}{\text{cm}^2} \quad . \tag{11}$$

*J. Randolf and J. Morrison, "Rayleigh-Equivalent Resolution of Acousto-optic Deflection Cells," Applied Optics, Vol. 10, No. 6, p. 1453, 1971.

4.2 Continued

Similar measurements were performed for the blue optical signal beam to obtain a first order diffraction signal beam intensity distribution $I_{SB}(x,y)$ of the PROM surface for a single frequency input signal of:

$$I_{SB}(x,y) \cong \left(\frac{DE}{100\%}\right)(.10)e^{-\left(\frac{y}{0.1}\right)^2} e^{-\left(\frac{x-x_o}{0.0027}\right)^2} \quad \frac{Watts}{cm^2} \tag{12}$$

Note that the spatial distribution of the blue beam matches that of the red beam as intended. Also, the blue beam is 5.6 times less intense than the red beam.

Finally, the intensity of the red reference beam $I_{RR}(x,y)$ at the PROM surface was also measured in a manner similar to the above estimates. The result is:

$$I_{RR}(x,y) \cong \left(1.5 \times 10^{-4}\right) e^{-\left(\frac{y}{0.07}\right)^2} \quad \frac{Watts}{cm^2} \tag{13}$$

As before, the 1/e intensity width at 0.14 centimeters in the y direction was obtained by a visual estimate.

Using Equation 13, the maximum exposure per square centimeter for the red reference beam for a 5-second period is given by 7.5×10^{-4} joules/cm^2. Using the 1/e voltage decay exposure of 10^{-3} joules/cm^2 for the PROM at 6328 A (as quoted by Itek), this predicts a maximum voltage decay at $e^{-.75} = .47$ due to the reference beam after 5 seconds of exposure. In actual experimentation with

4.2 Continued

the blue write beam blocked and a low-level, broadband signal input which produced an optical signal beam intensity much weaker than the red reference beam intensity, the detected signal decayed to approximately 60% of its original amplitude after 5 seconds from the start of the read stage. This decay is due to the red reference beam and is in moderately close agreement with the decay to $\sin^2\left[\frac{\pi}{2}(.47)\right] \times 100\% = 45\%$ which is predicted by the above calculation. The moderate difference between the experimental result and the predicted result can be at least partly attributed to the fact that the prediction was for the maximum amount of voltage decay at the center of the gaussian in Equation 13 as opposed to an "average" decay over the entire reference beam width which occurs in the experimental measurement.

For time periods much less than 5 seconds, the red reference beam causes negligible voltage decay across the PROM so that the voltage decay is dominated by the red and the blue signal beams. One can formulate the peak voltage decay across the PROM for a single frequency input with a blue exposure time of $(t-t_0)$ seconds using the fact that the 1/e decay exposures for red and blue are 10^{-3} and 4×10^{-6} joules/cm^2, respectively. The peak exposure occurs at $y = 0$ and $x = x_0$ so that from Equations 11 and 12 one can derive:

$$\text{Peak Voltage Decay} = e^{-\left(\frac{DE}{100\%}\right)\left[\frac{(0.1)(\Delta t)}{4 \times 10^{-6}} + \frac{(.56)\left(t-t_0\right)}{10^{-3}}\right]} \qquad (14)$$

$$= e^{-\left(\frac{DE}{100\%}\right)\left[25{,}000\Delta t + 560\left(t-t_0\right)\right]}$$

, $t \ll 5$ seconds

4.2 Continued

Thus with the blue write beam blocked, a single frequency diffraction efficiency of 0.18% should create a 1/e peak voltage decay after $(t-t_0)$ = 1 second due to the red signal beam. Similarly, with a single frequency diffraction efficiency of 0.004%, the blue beam should create a 1/e peak voltage decay after a blue exposure time Δt = 1 second.

4.3 FREQUENCY RESPONSE WITH A SINGLE TONE EXCISION NOTCH

One experiment which was performed to examine the PROM for its capabilities as an excisor of narrowband interference was to use a single frequency tone for the input signal during the write signal stage of the PROM cycle and then use a network analyzer to measure the acousto-optic system's RF frequency response during the read stage. The test configuration for this set of measurements is shown in Figure 4-3. During the write stage, the acousto-optic system's RF input is switched to a single frequency input at 40 MHz which generated an acousto-optic modulator input level of 8 volts peak to peak or a 12.1% first order diffraction efficiency. This single tone during the write stage will cause the blue write beam to expose a spot on the PROM and create a frequency excision notch at 40 MHz. During the read stage, the acousto-optic system's RF input was switched to an HP 8505A network analyzer which displayed the system frequency response on a CRT. The signal level of the frequency chirp used by the network analyzer was at a low level to prevent any decay of the PROM voltage caused by the red read signal beam. A series of photographs of the system frequency response during the read stage were taken for several blue write time durations Δt. These photographs are shown in Figures 4-4A through D, where Δt = 0.05, 0.15, 0.3, and 0.6 seconds for A, B, C, D, respectively. Larger values at Δt did not create any significant change in the excision notch depth so that Δt = 0.3 seconds appeared to be a long enough time duration to achieve a maximum excision depth (approximately 30 dB). For comparison purposes, an optically-opaque wire was placed in the Fourier transform plane to act as an excision notch. The frequency response with this wire excision is shown in Figure 4-5. Note that even with a perfectly opaque, moderately thick wire, it was not possible to obtain an excision depth greater than 42 dB.

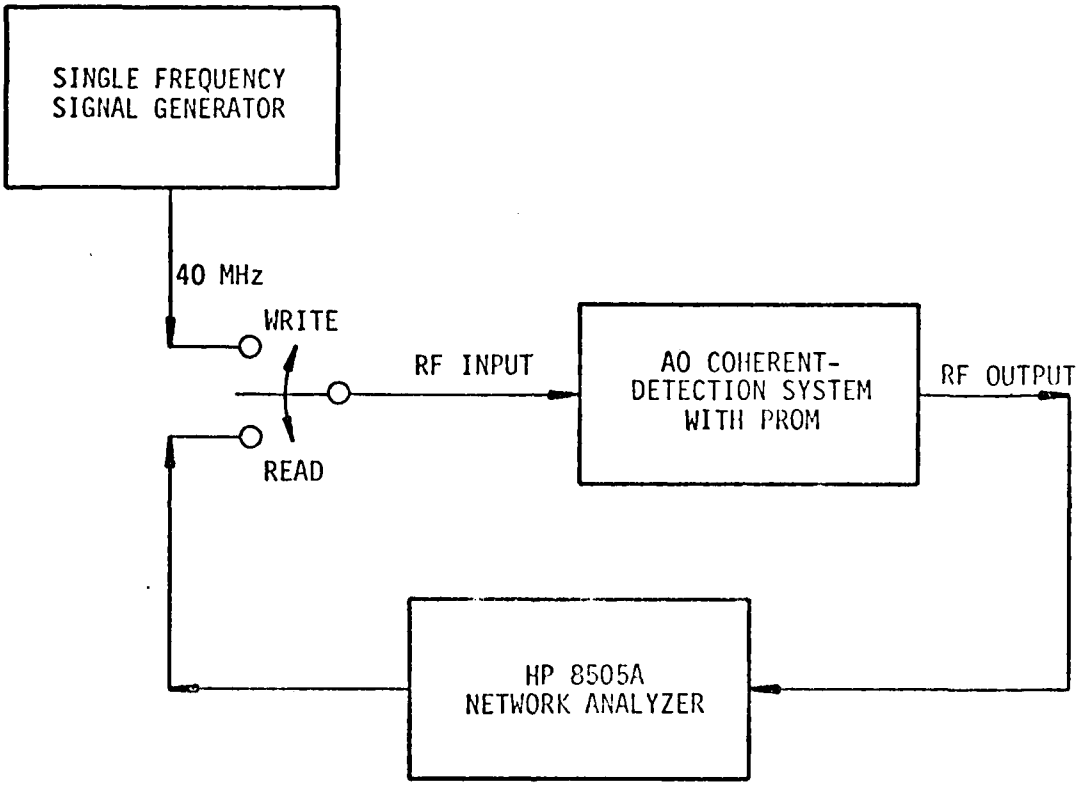

PSI-80066

FIGURE 4-3

TEST CONFIGURATION FOR MEASURING THE AO SYSTEM
FREQUENCY RESPONSE WITH A SINGLE FREQUENCY EXCISION NOTCH

VERT: 10 dB/Div
HORIZ: 3.3 MHz/Div

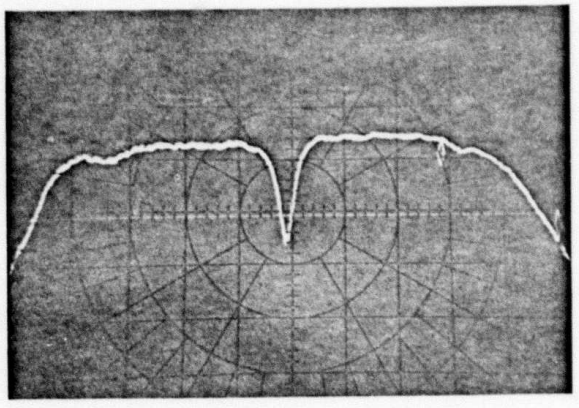

A. BLUE WRITE TIME Δt = 0.05 SEC

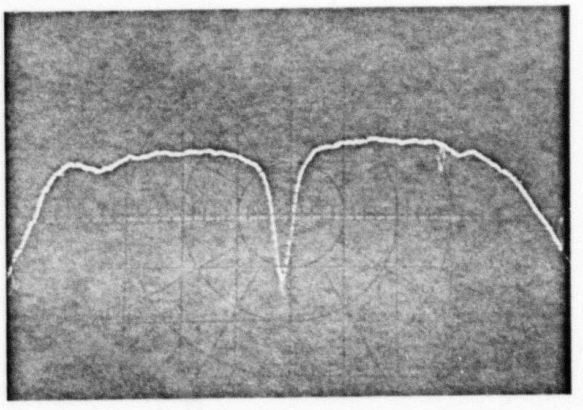

B. Δt = 0.15 SEC

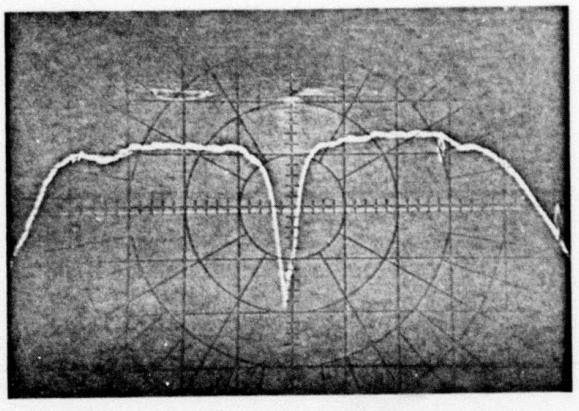

C. Δt = 0.30 SEC

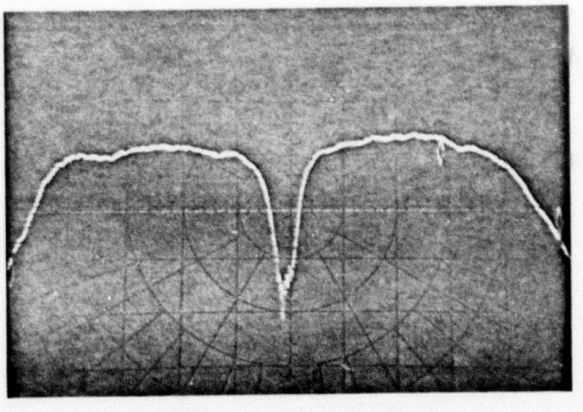

D. Δt = 0.60 SEC

FIGURE 4-4 FREQUENCY RESPONSE WITH A SINGLE TONE EXCISION NOTCH

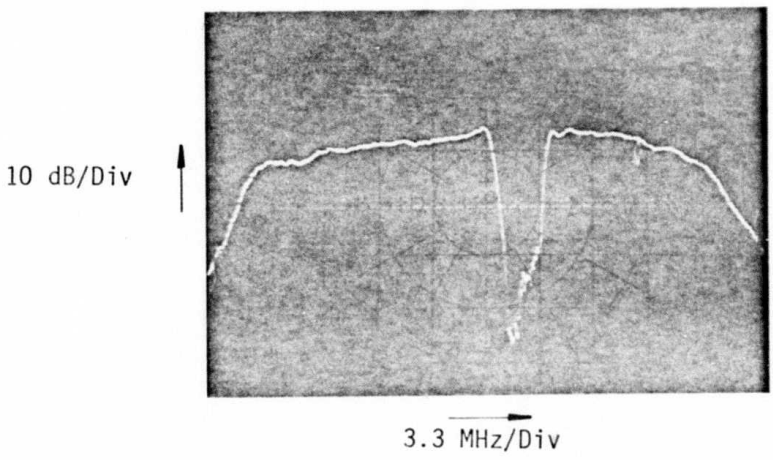

FIGURE 4-5

FREQUENCY EXCISION USING AN OPTICALLY OPAQUE WIRE
IN THE PROM ACOUSTO-OPTIC SYSTEM

4.3 Continued

Also, the excision notch is lopsided. In theory, with smooth Gaussian illumination at the acousto-optic modulator, the excision notch for Figure 4-5 should be much deeper and more symmetrical. The cause of the degraded notch shape is believed to be the mild ripple in the illumination at the acousto-optic modulator, as previously explained in Section 4.2. Thus, it does not appear that the PROM is the fundamental limit for the excision depth for the photographs in Figure 4-4. Rather, an undesirable optical reflection from a non-antireflection coated cylindrical lens appears to create an uneven acousto-optic modulator illumination and thereby limit the excision depth.

One should also note in examining the excision notches at Figure 4-4 that the notch width is relatively wide in relation to the total bandwidth. It appears that one could have approximately 10-15 individual excision notches across the 25-MHz bandwidth, while the 3-dB time-bandwidth product previously calculated in Section 4.2 is 46. Part of the reason for the wide excision notches in Figure 4-4 is believed to be the finite spatial resolution at the PROM. According to the "PROM Evaluation Test Report" distributed by Itek, the PROM modulation transfer function or MTF drops to roughly 50% at 10 lines/millimeter, while the signal beam 1/e intensity width for the Gaussian spot in the Fourier transform plane is approximately 0.045 millimeters. Thus, the Gaussian spot size could not be accurately resolved by the PROM. This theory is supported by examining Figure 4-5, which shows steeper excision notch edges using a wire than the PROM excision notches of Figure 4-4.

4.4 SINGLE FREQUENCY INPUT VERSUS OUTPUT POWER

To further examine the narrowband signal rejection characteristics at the PROM acousto-optic system, data was taken on the input signal power versus output power using a single frequency signal. A blue write time of $\Delta t = 0.3$ seconds was used for this data, while the single frequency input and output power levels were read from a spectrum analyzer display. This data is plotted in Figure 4-6, where the solid line represents the single frequency detected output, while the dotted line represents the single frequency acousto-optic diffraction efficiency

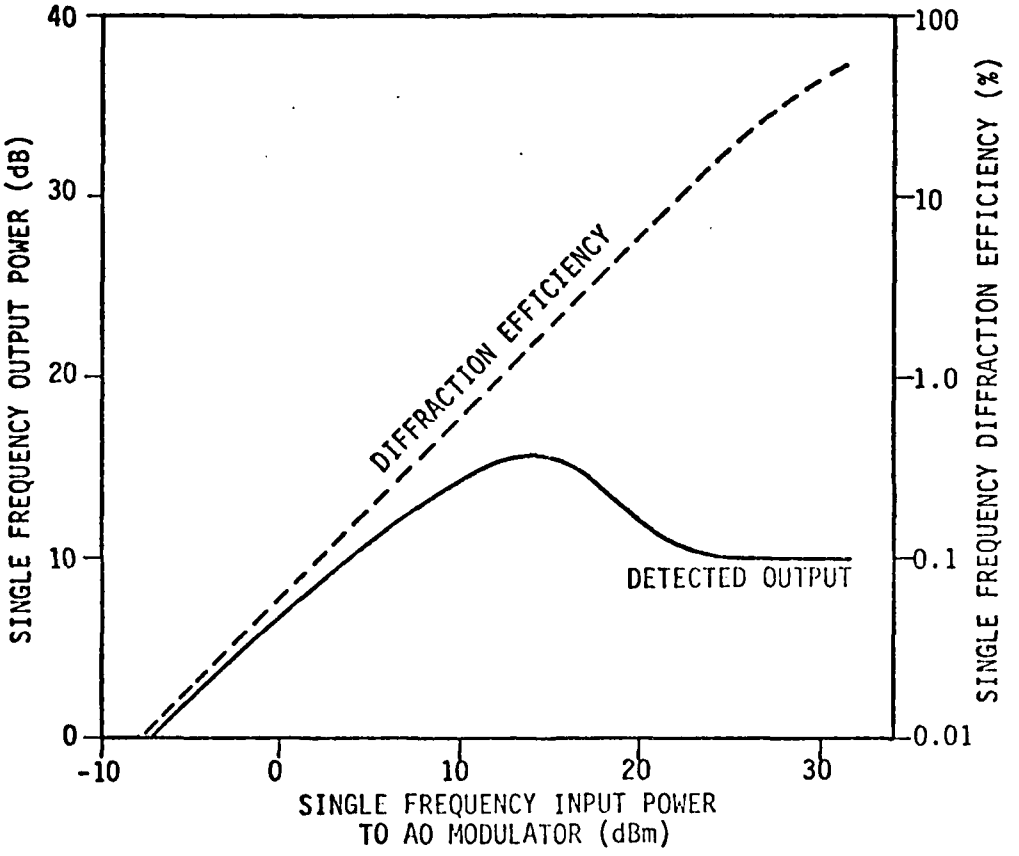

PSI-80067

FIGURE 4-6

EXPERIMENTAL DATA FOR PROM CLIPPING CHARACTERISTICS WITH
A SINGLE FREQUENCY INPUT AND A BLUE WRITE TIME AT Δt = 0.3 SEC

4.4 Continued

into the first order. The difference between these lines represents the single frequency attenuation created by the PROM, which is seen to attain a value of 27 dB at an input signal power of 31 dBm.

If one compares Figure 4-6 with the mathematical prediction of Figure 2-2, one sees that actual single frequency output power does not decrease as rapidly as the predicted decrease for high signal levels. This can be partly explained by the fact that the plot of Figure 2-2 represents a peak attenuation as opposed to a spatially averaged attenuation of the diffracted signal beam on the PROM surface. Also, the spurious optical reflection previously described in Sections 4.2 and 4.3 is a probable cause for the limited single frequency excision depth. However, both the mathematical predictions and experimental results show that the PROM as an optical clipper will create a maximum output level such that stronger input signals can actually be weaker in output power than a weaker input signal. This is a desirable property for many narrowband rejection applications.

4.5 EXCISION WITH WIDEBAND NOISE PLUS NARROWBAND INTERFERENCE

To exemplify the ability of the PROM-based acousto-optic system to excise narrowband interference yet pass broadband signals, a signal consisting of broadband noise plus a single frequency tone was used as the input to the acousto-optic system. The PROM was then cycled between the write and read stages with a blue write time at $\Delta t = 0.3$ seconds. The coherently detected output at the acousto-optic system during the read stage was then displayed on a spectrum analyzer and compared to the input spectrum. Photographs of the input signal spectrum are displayed in Figures 4-7A, C, and E, while the corresponding coherently detected outputs are shown in Figures 4-7B, D, and F, respectively. For all of the photographs, the spectrum analyzer was set for a 300-kHz bandwidth and the input single frequency power to noise power remained constant. For Figures 4-7A, C, and E, the input single frequency power is 11, 21, and 31 dBm, respectively, while the noise power is approximately 0, 10, and 20 dBm, respectively, for a 20-MHz bandwidth. Thus, the single frequency power to noise power ratio for

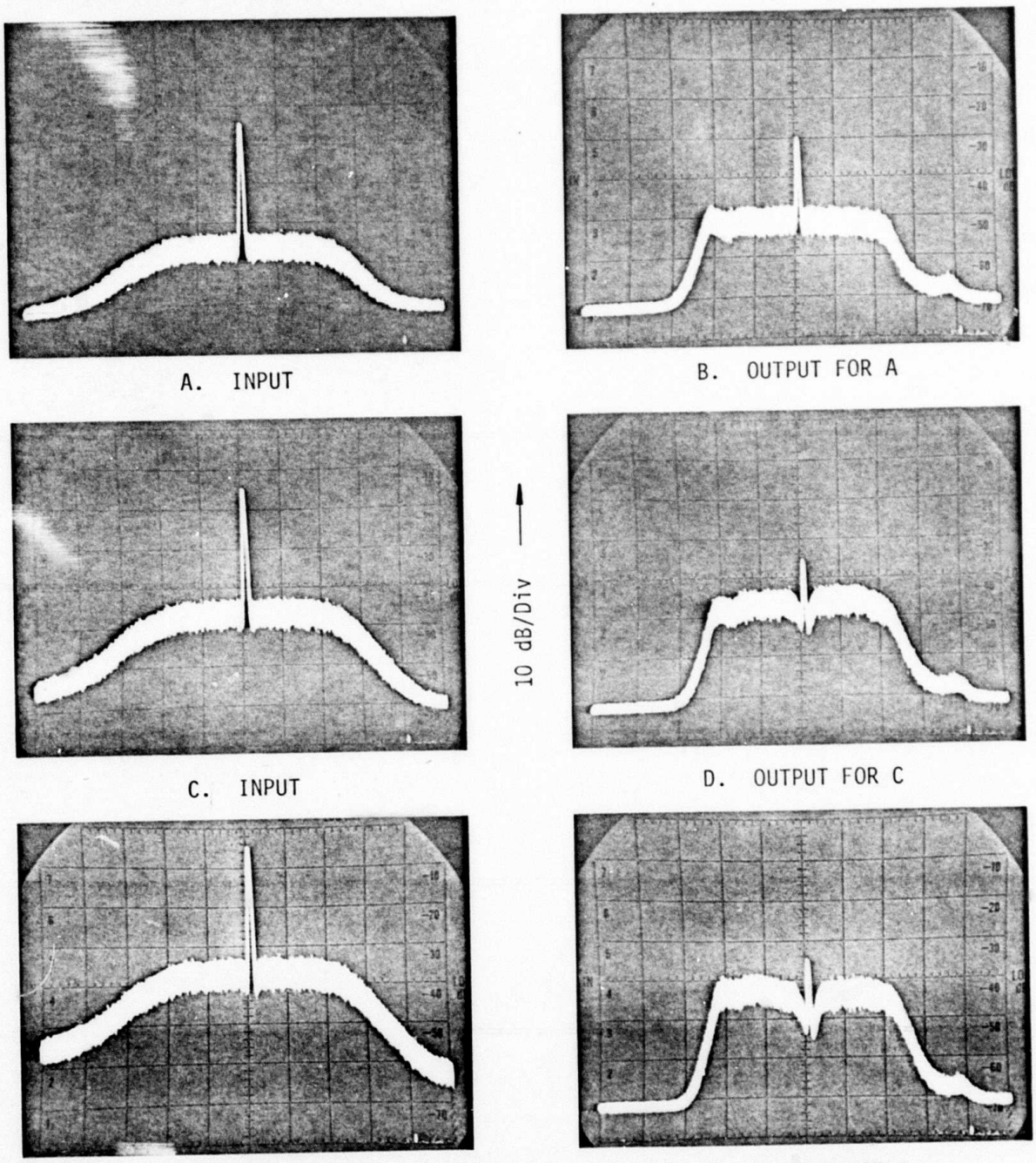

FIGURE 4-7

EXCISION WITH WIDEBAND NOISE PLUS A SINGLE FREQUENCY FOR THE INPUT

4.5 Continued

a 20-MHz bandwidth is approximately 11 dB for the input signal. For the output at Figure 4-7B, the noise level is only 3 dB above the photodetector shot noise level so that the actual noise level due to the input signal noise should be 3 dB less than indicated. Thus, the output single frequency power to noise power ratio for Figure 4-7B assuming a noiseless photodetector and 20-MHz bandwidth is approximately 3 dB, or 8 dB less than the input ratio. For Figure 4-7D, the output single frequency power to noise power ratio for 20-MHz bandwidth is reduced to -10 dB, while for Figure 4-7F, the ratio is reduced to -12 dB. Thus, a 23-dB decrease in the single frequency power to wideband noise power ratio can be achieved with the PROM-based acousto-optic system.

It is interesting to note that a 10-dB increase in the wideband noise power at the input did not result in a 10-dB increase in the noise power at the output. After subtracting 3 dB from the noise level at Figure 4-7B to account for the photodetector noise, the output wideband noise power from Figure 4-7B to Figure 4-7D increased only 8 dB. Similarly, the output wideband noise power from Figure 4-7D to 4-7F increased by only 3 dB. Apparently the noise power level at the input of Figure 4-7C and 4-7E is sufficient to cause some attenuation of the noise as well as the single frequency tone. This explains why only a 23-dB improvement in the single frequency power to noise power ratio is obtained, as opposed to the 27-dB rejection of narrowband interference obtained in Section 4.4.

4.6 EXCISION WITH NO BLUE WRITE LIGHT

As previously discussed in Section 2, it is not necessary to utilize any blue light for the PROM write stage for optical clipping since the red readout beam will act to write an image of itself and thereby cause self-attenuation of the red readout beam. This self-attenuation, as expressed in Equation 9, occurs more rapidly for the intense portions at the red readout beam so that strong narrowband interference will be attenuated more rapidly.

The major difference between writing with the blue beam versus the red readout beam is that the red readout beam will erase itself much slower. To

4.6 Continued

test this mode of operation the blue write beam was blocked and the PROM was cycled through its write and read stages as before. An input consisting of a single frequency at 40 MHz was used, and the detected output of the optical system was displayed on a scope with a slow sweep to observe the output magnitude versus time. Photographs of this detected output magnitude versus time are shown in Figures 4-8A and 4-8B. For Figure 4-8A, the first order diffraction efficiency was 12% and resulted in a 1/e decay time at approximately 0.3 seconds. For Figure 4-8B, the first order diffraction efficiency was 3% and resulted in a 1/e decay time of 1.3 seconds.

Since the red read beam intensity is inversely proportional to the decay time as predicted by Equation 9, the decay time for the single tone at 3% diffraction efficiency should be four times the decay time for the single tone at 12% diffraction efficiency. This compares well with the ratio $1.3/0.3 \cong 4.33$ obtained from Figures 4-8A and 4-8B. However, the magnitude decay versus time does appear to follow the same form as Equation 9 would predict with uniform illumination. Equation 9 predicts that the output level would be constant for a sort period of time at the beginning of the read cycle with $V_0 = V_H$ and uniform illumination. No such constant level can be found in Figures 4-8A or 4-8B. This can be explained, at least partially, by the Gaussian distribution as opposed to a uniform distribution so that the peak at the Gaussian will decay much more rapidly than its tails.

Equation 14 in Section 4.2 predicts a $1/\sqrt{e}$ voltage decay time for the center of the Gaussian signal beam at a 12% diffraction efficiency of 0.0074 seconds. If the approximation $\sin^2 x = x^2$ is used, the $1/\sqrt{e}$ voltage decay time equals the 1/e optical intensity decay time and Equation 14 predicts an optical intensity 1/e decay time of 0.0074 seconds, which is approximately 40 times faster than the 0.3-second value obtained from Figure 4-8A. Thus, the peak at the Gaussian should decay much faster than the average decay data in Figure 4-8 suggests.

The extreme discrepancy (a factor of 40) between the calculated peak decay rate and the average decay rate could be due to one or more effects. If the

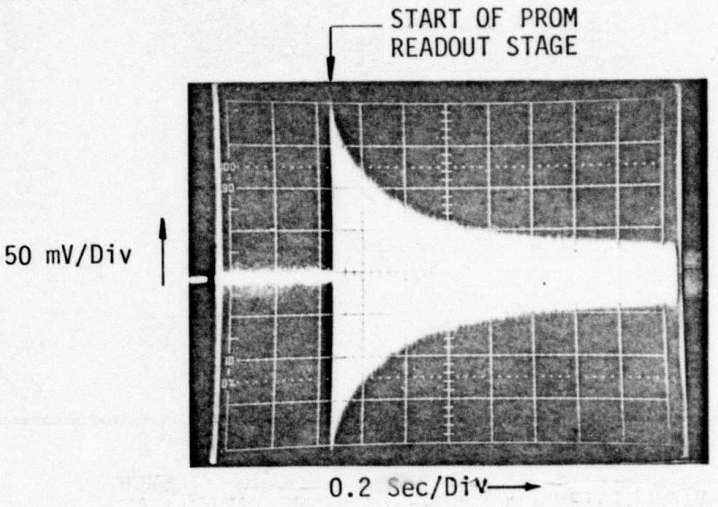

A. FIRST ORDER DIFFRACTION EFFICIENCY AT 12%

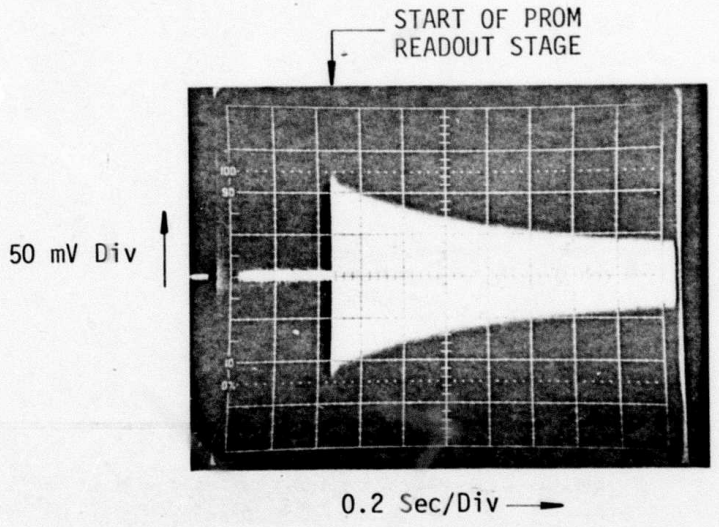

B. FIRST ORDER DIFFRACTION EFFICIENCY AT 3%

FIGURE 4-8

DETECTED OUTPUT MAGNITUDE VERSUS TIME FOR A SINGLE FREQUENCY INPUT WITH NO BLUE WRITE LIGHT IN PROM CYCLE

4.6 Continued

calculation of the Fourier transform plane intensity distribution is assumed to be correct, then the task is to calculate the transmittance as a function of time for each x and y in the two-dimensional Gaussian-shaped illumination pattern. Not only is this calculation a non-trivial effort, but the accuracy of the theoretical model is degraded by any factors which could reduce the resolution of the incident and transmitted light. For example, a slight misfocusing of the Gaussian spot would cause a corresponding decrease in optical intensity. There may also be spreading effects in the PROM iteslf since the PROM modulation transfer function, of MTF, decreases to roughly 50% at 10 lines per millimeter, while the signal beam 1/e spot width is calculated to be 0.054 millimeters.

4.7 CORRELATION WITH A JAMMING SIGNAL AND OPTICAL EXCISION

To demonstrate that the PROM-based acousto-optic system can perform excision of narrowband interference from a wideband signal, a digital code generator and correlator was tested with the system. As in previous experiments, the PROM was cycled between the record and readout stages with a blue write time of $\Delta t = 0.3$ seconds. The input signal consisted of wideband noise plus a single frequency jamming signal at 42 MHz plus a 40-MHz carrier bi-phase modulated at a 10-MHz rate by a repeating 127-bit digital code. For more details on the digital code and digital correlator see PROBE's report on the microchannel plate photo-multiplier (Report PSI-ER-5538-02). This input was filtered to a 23-MHz bandwidth centered at 40 MHz before entering the acousto-optic system. The signal power of the digital code was set to be 4 dB below the power of the wideband noise so that the input SNR was -4 dB.

The combined input signal was passed through the PROM-based acousto-optic system, downconverted, and correlated with a digital matched filter. The probability of detection was then measured as a function of the input jamming to signal ratio (J/S). This probability of detection is plotted in Figure 4-9, where the solid line represents the data for the PROM-based acousto-optic system, and the dotted line represents the probability of detection with the PROM-based acousto-optic system replaced by a coaxial cable. The difference between the two curves can be attributed to the narrowband excision performed by the PROM system.

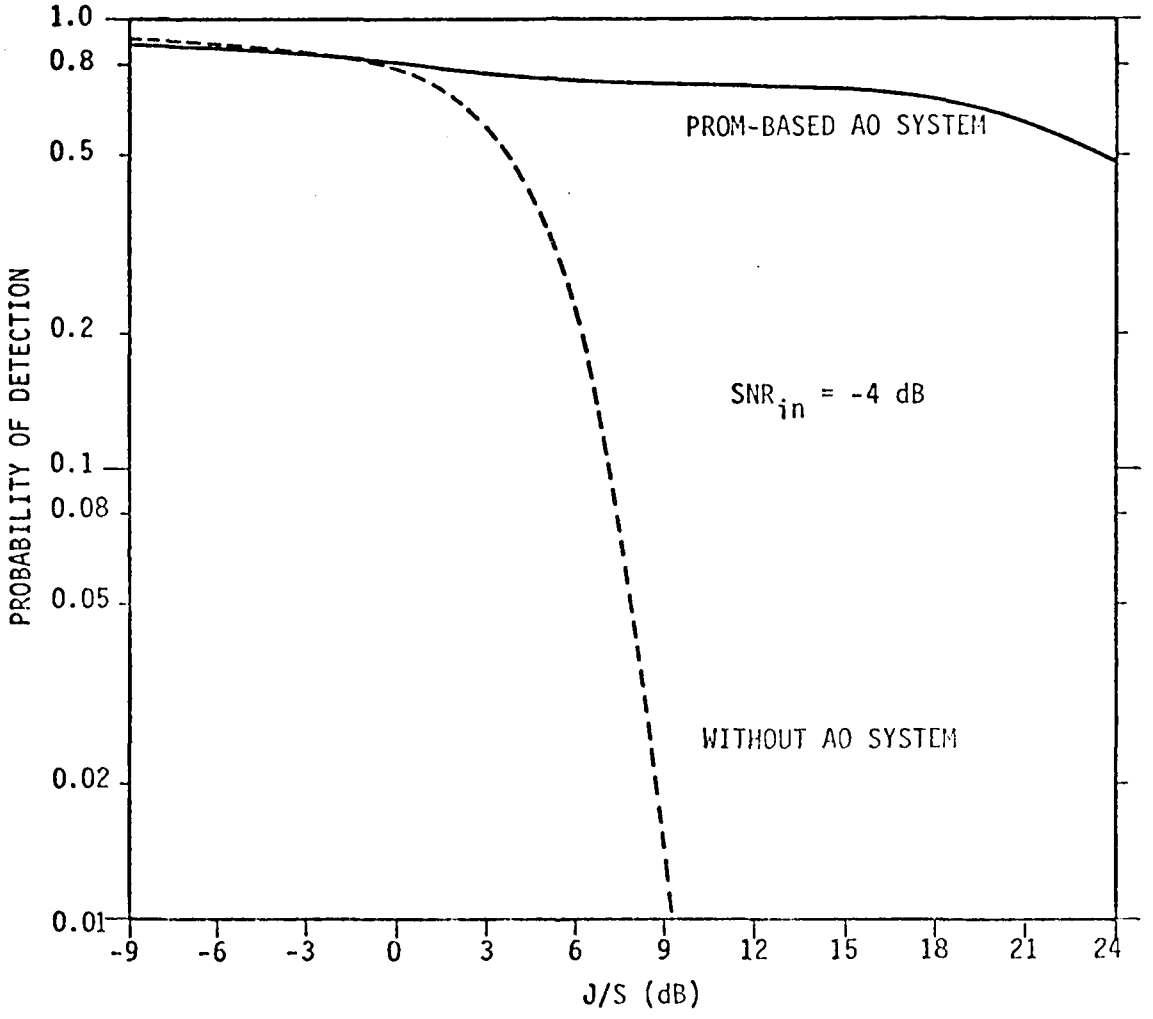

PSI-80068

FIGURE 4-9

PROBABILITY OF DETECTION FOR 127-BIT DIGITAL CORRELATOR
AS A FUNCTION OF J/S WITH INPUT SNR = -4 dB

4.7 Continued

It can be seen that the PROM system reduces the effects of a jammer by 20 dB even with a negative input SNR. J/S ratios higher than 24 dB could not be measured due to the power limits of the acousto-optic modulator.

4.8 EXCISION OF NARROWBAND INTERFERENCE FROM A PULSED SIGNAL

One final experiment was performed to demonstrate the ability of the PROM-based acousto-optic system to pass wideband signals yet excise narrowband interference. For this experiment, a single frequency interference signal was added to an RF pulse signal to create a combined input signal.

As in previous experiments, the PROM was cycled between the record and readout stages with a blue write time of $\Delta t = 0.3$ seconds. The RF pulse consisted of approximately nine cycles at a 40-MHz sine wave with a 1% duty cycle. The single frequency interference signal was at 46 MHz. The combined input signal is shown in the time domain in Figure 4-10A via a scope, and in the frequency domain in Figure 4-10B via a spectrum analyzer. After going through the PROM-based acousto-optic system the narrowband interference was excised, while the pulsed signal was passed. This excised output is shown in Figure 4-10C on a scope, and in 4-10D on a spectrum analyzer. Comparing Figures 4-10B and 4-10D, one can see that the narrowband interference was excised by about 27 dB relative to the pulsed signal.

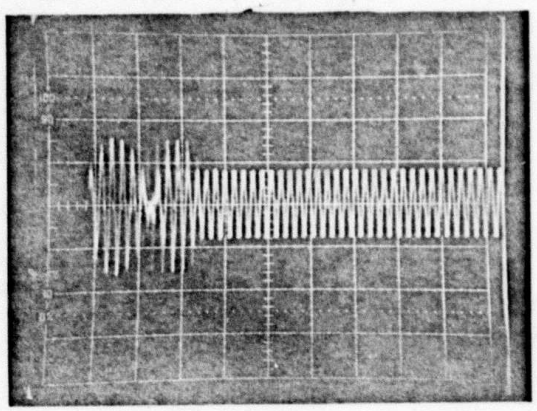

A. COMBINED INPUT ON A SCOPE

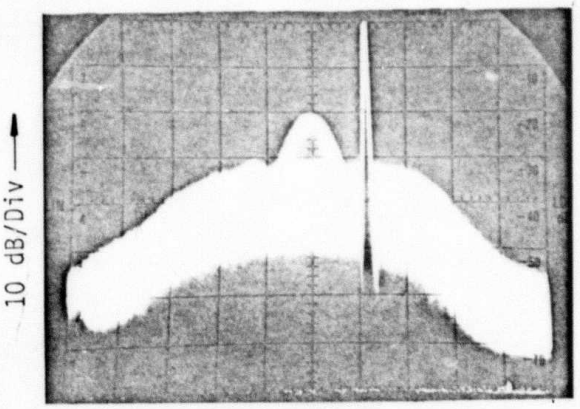

B. COMBINED INPUT ON A SPECTRUM ANALYZER

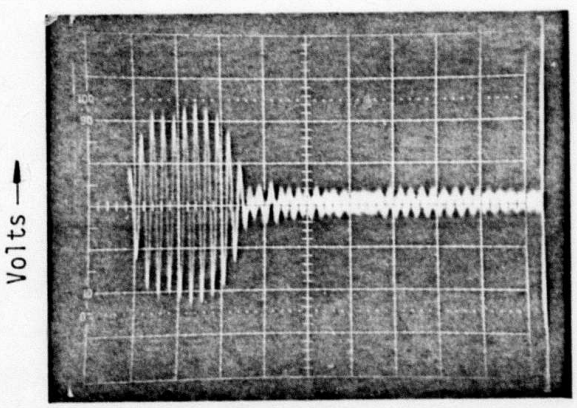

C. OUTPUT OF PROM BASED SYSTEM ON A SCOPE

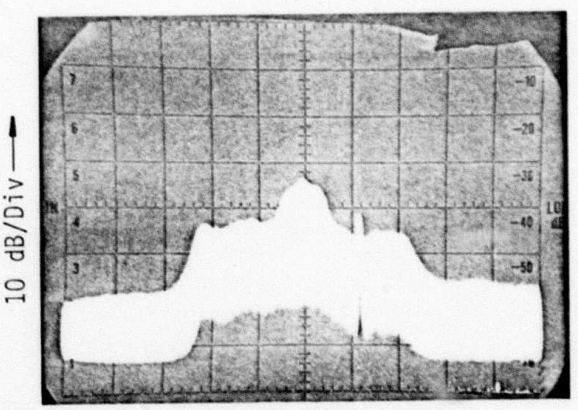

D. OUTPUT OF PROM BASED SYSTEM ON A SPECTRUM ANALYZER

FIGURE 4-10

EXCISION OF NARROWBAND INTERFERENCE FROM A PULSED SIGNAL

SECTION 5
PROM CONCLUSIONS

The results of the work reported here have demonstrated the feasibility of using a PROM in a coherent optical signal processor to automatically excise narrowband interference from a broadband signal. The processor formed the spectrum of the signal as a spatial distribution of light such that a broadband signal covers a relatively large region and a narrowband signal comes to focus to a small spot. The transmission through polarizers and the PROM was considerably less for the narrowband signal, and hence the strength of a narrowband jammer was reduced. For a spread spectrum signal, the PROM AO system provided at least 20 dB of anti-jam resistance via excision and permitted subsequent correlation of the spread spectrum signal. The potential antijam resistance may be much greater if the optical system is optimized to avoid optical reflections and the spatial resolution limits of the PROM.

There are two basic difficulties with incorporating the current version of the PROM in a real-time excision processor. The first difficulty stems from the fact that the PROM is designed as an optical image storage device instead of a real-time optical modulation device. This requires that one go through a write stage and a read stage, so that only the jamming signals present during the write stage will be excised during the read stage. This makes the PROM AO system highly vulnerable to jammers which are switched on and off.

Alternatively, one could consider a PROM system based on the self-attenuation effect at the read beam with a single laser. If the PROM were physically translated in the Fourier transform plane so that a new area of the PROM is continually exposed, the read signal beam could act to adaptively cancel the strong portions of the signal beam. However, even with a 2-mW blue laser for the read beam, the adaption time to excise a strong narrowband interference signal would be on the order of 0.1 seconds, which would be too slow for many applications. Also, the PROM would have to be repositioned periodically to the beginning of its translation position so that this mode of operation would not result in a true real-time system.

5. Continued

The second basic problem with incorporating the current version of the PROM in a real-time excisor is that it requires a significant amount of support electronics and optical components for its functioning. Even with a one-laser translating PROM system, the PROM control electronics, the required motor control electronics, and a blue argon laser would require considerable space, weight, and electrical power.

Despite the drawbacks of the current PROM as an optical clipper in a compact real-time processor, the many successes of the PROM in the laboratory environment suggest that a simple, real-time device similar in construction to the PROM may be feasible. The envisioned device is illustrated in Figure 5-1. The operation of this device would be the same as the PROM except that instead of capacitively storing the change image generated by the write light to spatially modulate the voltage distribution across the crystal, the spatial voltage distribution would be modified in real-time by resistively dividing the electrode voltage between the photoconductive crystal and the semi-resistive, transparent material. The more intense the incident light, the less the voltage across the crystal would be. Such a device could be designed to require virtually no support electronics other than a high voltage, very low current power supply. If the crystal were chosen to be photoconductive with red or infrared radiation, very compact HeNe or diode lasers could be used as the single laser source so that the final system would be very small, compact, and low in power consumption. Also, the adaption speed of such a device could be potentially very fast, depending on the photoconductivity of the crystal and the dielectric constants of the semi-resistive material and the crystal.

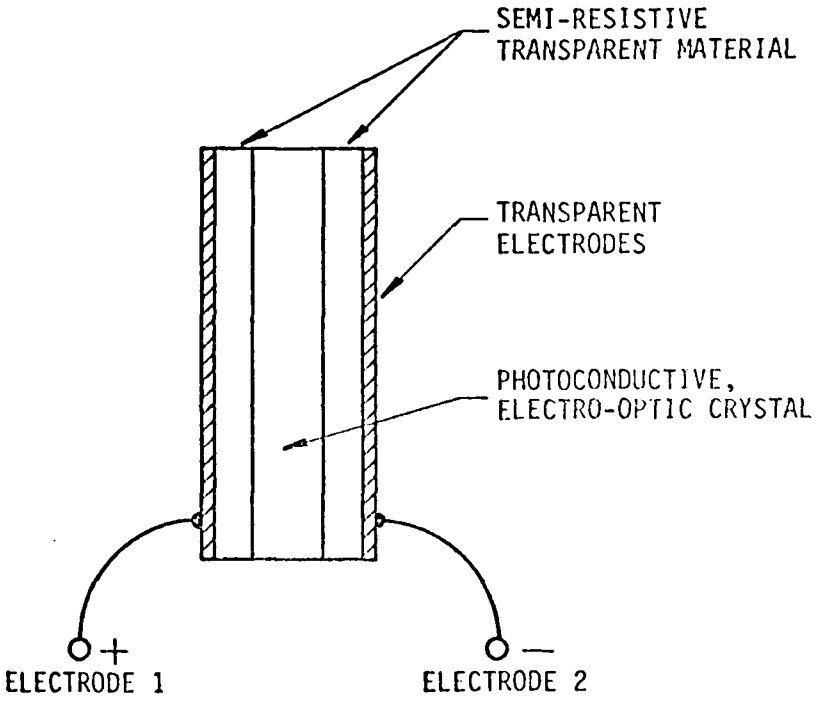

PSI-80069

FIGURE 5-1
ENVISIONED REAL-TIME DEVICE FOR OPTICAL EXCISION

SECTION 6
PHOTODICHROIC DESCRIPTION

6.1 INTRODUCTION

The work described in this section concentrated on the evaluation of photodichroic crystals as an optical clipper in an excisor. The basic approach is to place a crystal in the spectral plane of an optical spectrum analyzer and operate the crystal such that broadband signals would cause a low optical power density on the crystal and the crystal would remain polarized according to polarization of the optical bias light source. By arranging the input, output, and bias polarizers, it would then be possible to allow broadband signals to be rotated by the crystal and nearly a quarter of the input light to be passed to the detector.

A narrowband signal would be much higher in optical power density, and therefore override the influence of the bias light. The crystal would then be unable to rotate the polarization of the signal light, and hence the signal would be blocked before it reached the photodetector.

Figure 6-1 illustrates the operation of the photodichroic crystal as an optical clipper at the transform plane of a coherent optical processor. The input signal beam is diffracted by a Bragg cell and has an optical power distribution corresponding to the input RF power spectrum. A polarizer at the input to the clipper minimizes components of the input beam other than ones at the desired polarization.

The crystal, located at the spectrum focal plane, is illuminated by two optical sources: the input signal beam and the optical bias light source. The bias source is polarized along the axis of the crystal. Bias illumination tends to polarize the crystal along its own axis. The signal beam which has a polarization bisecting the crystal axis tends to randomize the defects in the crystal, causing the polarization to be changed by an amount proportional to the intensity.

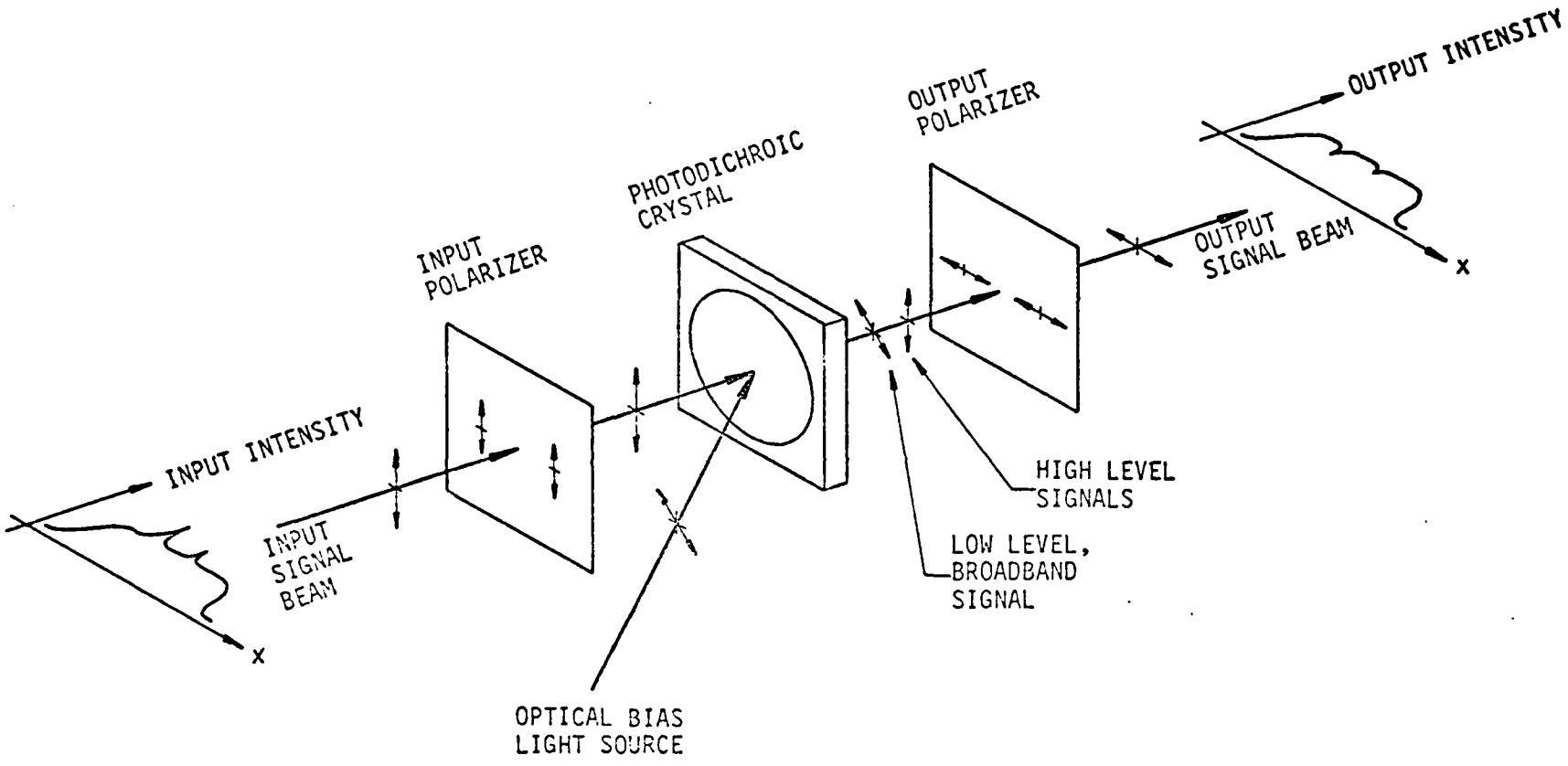

FIGURE 6-1

PHOTODICHROIC CRYSTAL AT THE TRANSFORM PLANE OF AN OPTICAL SPECTRUM ANALYZER

6.1 Continued

Now the optical power spectrum on the output polarizer has a polarization which is related to the spatial power distribution of the input spectrum and this polarizer (or analyzer) attenuates the signal beam based on its polarization. Weak signals in the spectrum are transmitted, while those at higher power densities are attenuated, which is illustrated in the input and output intensity plots shown in Figure 6-1.

Prior work* in Government laboratories with similar crystals has indicated that the crystals developed for the PROBE experiments would have the performance desired for a coherent optical excisor. The photodichroic crystals tested were KCl:LiCl and were supplied by the Naval Research Laboratory. After the crystals were cut and polished they were sandwiched between thin optical glass flats and sealed since they are hydroscopic. Before shipment to PROBE they were exposed to ionizing radiation by NRL to form the F centers†. Each were then activated (the process of forming F_A centers from the F centers) at PROBE by exposing the crystal with blue-green light. After activation the crystal was cooled to approximately 200° K with a closed-cycle cyrogenic cooler. This temperature was maintained throughout the testing since the crystals quickly degrade at room temperature.

6.2 OPTICAL ATTENUATION

The first experiments performed on the photodichroic crystals were to evaluate the attenuation properties of this candidate optical clipper. In these experiments, attenuation as a function of time was measured with uniform illumination on the crystal. These tests were performed at the optical power

---

*Collins, W.C. and Marrone, M.J., "Photodichroic Materials as Adaptive Spatial Filters in Real-Time Optical Spectral Analysis," *Applied Physics Letters*, Vol. 28, No. 5, p. 260 (1 March 1976).

†F centers and F_A centers are the defects in the crystal lattice that result in the dichcoism property. The physics of the material is explained in "Optical Recording Characteristics of KF:LiF Photodichroic Crystals," by Collins, Marrone, and Gingerich, NRL Report 8168.

6.2 Continued

densities expected for both spread and interfering signals at the transform plane of a coherent detection excisor. In another test, the crystal was placed at the transform plane of a processor configured for detection of the power spectrum. In this test, the power spectrum was coherently detected after imaging through the crystal.

6.2.1 Measurements With Uniform Illumination

The test setup for measurement of optical attenuation as a function of time for uniform illumination is shown in Figure 6-2. A vertically polarized helium-neon laser with an output wavelength of 632.8 nm illuminated an area of the crystal defined by 1-mm diameter aperture placed in the write beam path. Optical power through the input polarizer, crystal, and output polarizer was montiored with a Varian VPM152 PMT and recorded on a Honeywell oscillograph. An argon ion laser operating at a wavelength of 514.5 nm and polarized at a 45^{o} angle was used to initially polarize the photodichroic crystal and was switched off immediately prior to exposure with the write beam. The power density of the argon laser beam was 1 mW/cm^2 and the exposure time was long enough to allow the crystal transmission characteristic to attain a steady state value. Crystal temperature was maintained at 190^{o} K throughout the experiment. Laser power and polarizer attenuation were measured prior to each test run.

Typical attenuation data taken in tests with uniform illumination is plotted as a function of time in Figures 6-3 and 6-4. Figure 6-3 is for an incident optical density of 13 mW/cm^2 and shows an initial insertion loss of 18.4 dB. The optical power drops to P_o/e^2 (i.e., by 86%) in approximately 2.5 seconds. At 20 seconds the attenuation is 33.8 dB, which is within 1 dB of the 33-dB attenuation measured for crossed polarizers and represents a total change in transmission as a function of time of 15.4 dB. Figure 6-4 shows results obtained at the higher optical power density of 130 mW/cm^2. Increasing the power density by a factor of 10 has decreased the time required for the crystal to reach the P_o/e^2 value to about 0.4 seconds. As was the case for the data in Figure 6-3, the asymptotic attenuation value was within 1 dB of the 37 dB measured for crossed polarizers prior to taking data.

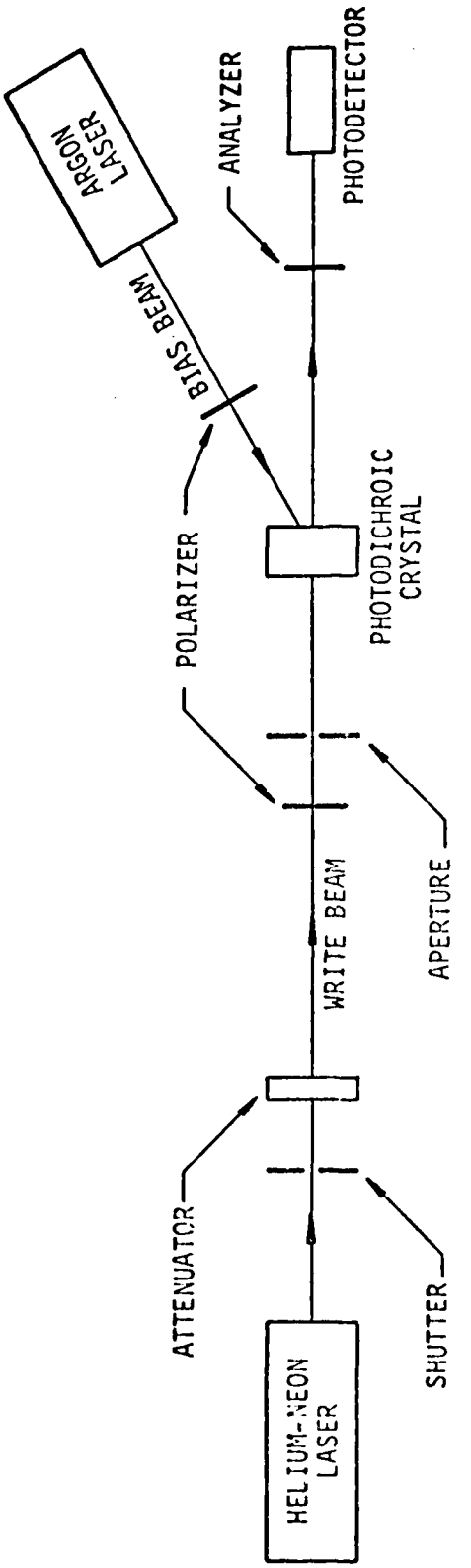

FIGURE 6-2 ATTENUATION TEST SETUP FOR UNIFORM ILLUMINATION

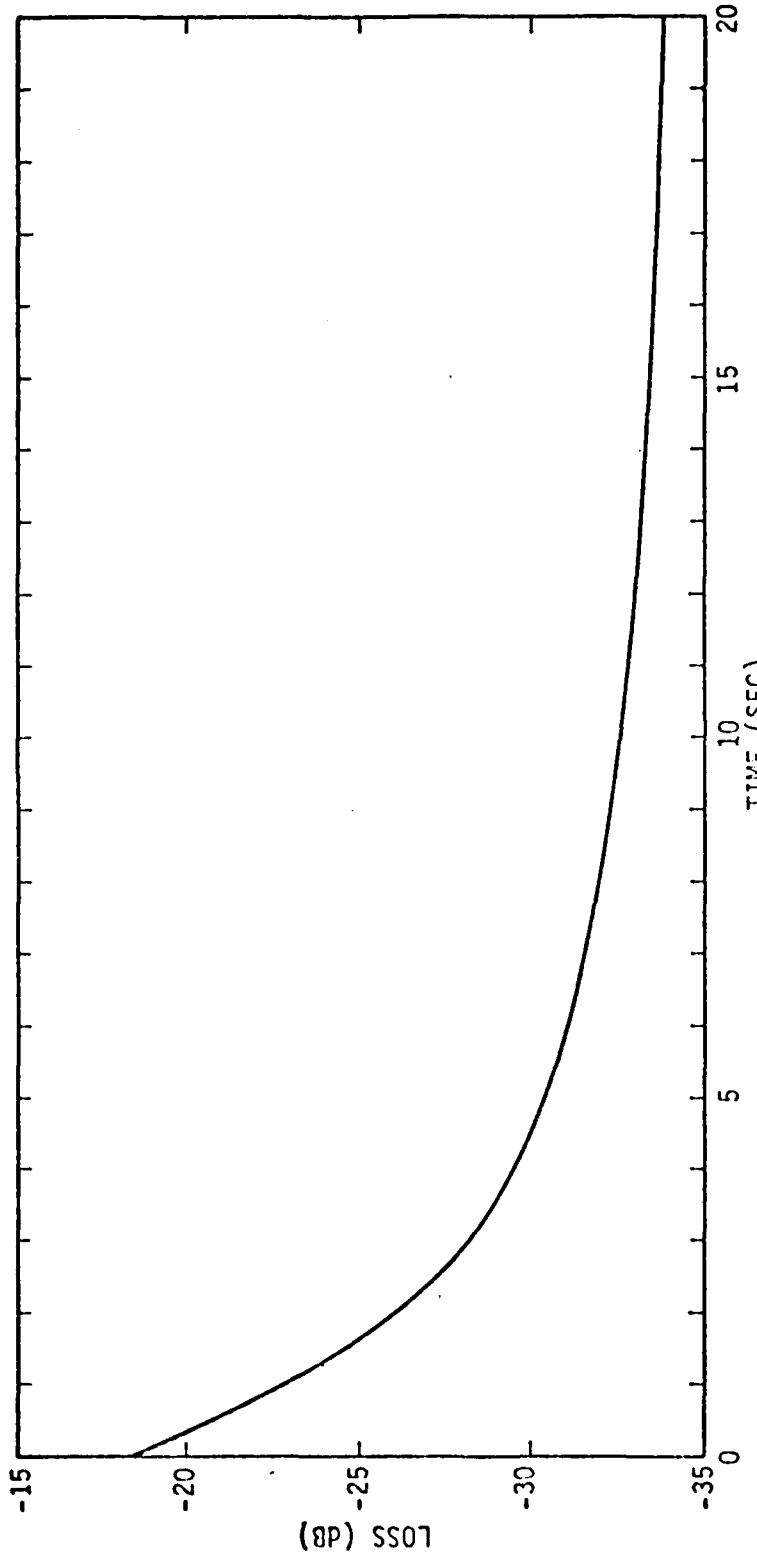

FIGURE 6-3

PHOTODICHROIC CRYSTAL -- INSERTION LOSS VS. EXPOSURE TIME FOR 13 mW/cm^2 INCIDENT OPTICAL POWER

PSI-00091

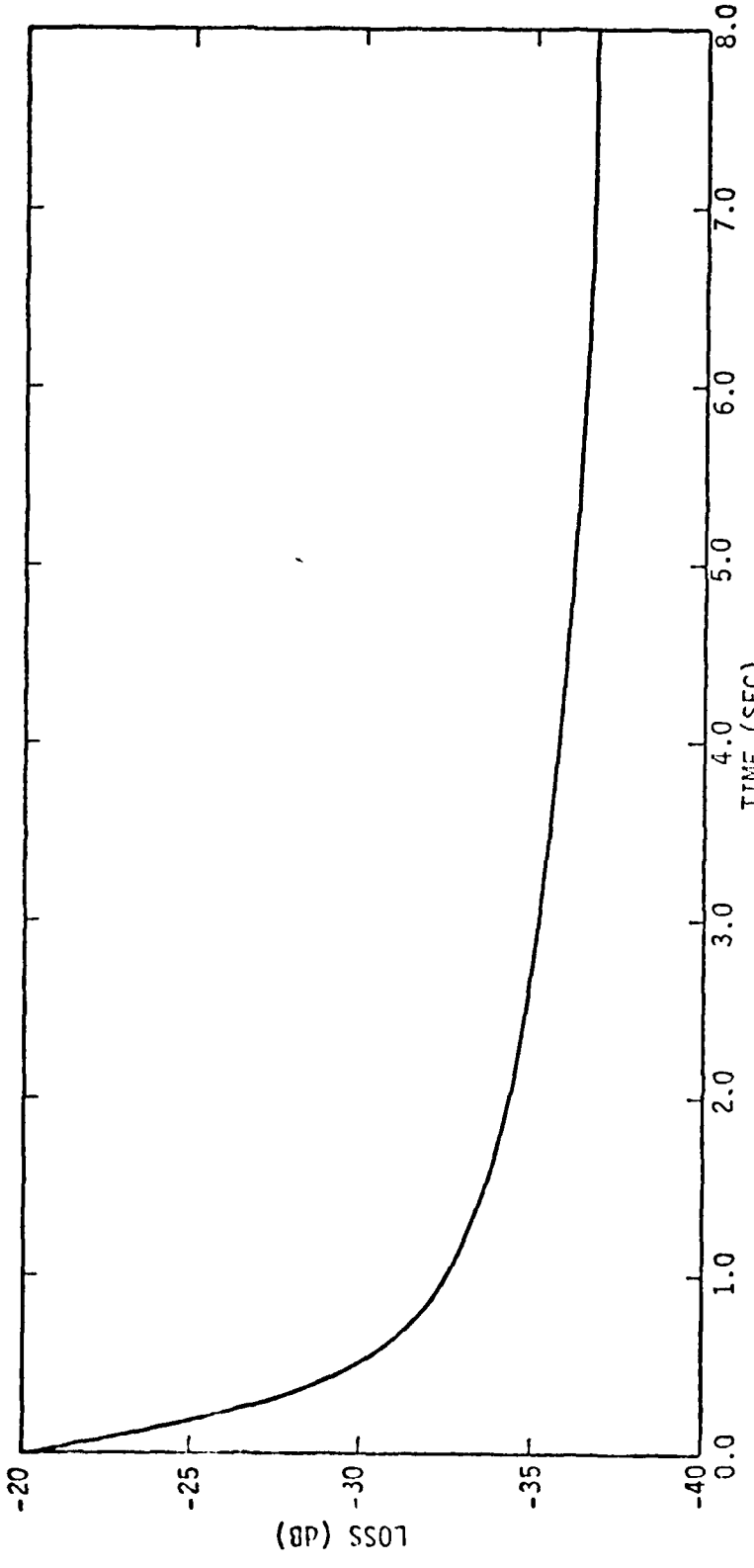

FIGURE 6-4
PHOTODICHROIC CRYSTAL -- INSERTION LOSS VS. EXPOSURE TIME FOR 130 mW/cm^2 INCIDENT OPTICAL POWER

PSI .92

6.2.2 Measurements With Diffracted Signal Illumination

In a coherent optical signal processor the illumination of the optical clipper is actually a two-dimensional Gaussian pattern (Section 4.2) and a series of measurements were made to directly determine the transmission of the photodichroic crystals when illuminated by the signal diffracted by a Bragg cell. The experimental setup (Figure 6-5) included some additional elements to accommodate the polarization properties of the crystals. Because the photodichroic crystal is placed between crossed polarizers, the light passed by the crystal is rotated by 90^{o}. In coherent detection the polarization of the signal beam must match the polarization of the reference beam and therefore a quarter-wave plate and a polarizer were placed in the reference beam path to rotate the reference polarization to that of the light passing through the crystal.

In these measurements, the output of the photodetector was measured with a spectrum analyzer, an oscilloscope, and a multimeter, for both the RF and DC signal content. With a narrowband RF input signal (typically a CW tone at about 70 MHz), the difference between the initial loss and the final loss of the crystal was about 23 dB as measured by the spectrum analyzer on the 70-MHz output component. The direct current measurements confirmed that the crystal could provide a reasonably high contrast of more than 12 dB. However, the maximum output signal-to-noise ratio at 70 MHz in a 30-kHz noise bandwidth was only 30.5 dB, which was about 20 dB below the maximum that was possible before the crystal was installed.

To determine the causes for this high insertion loss, the crystal was removed and an inexpensive sheet polarizer was inserted in its place. When the polarizer was rotated to simulate the crystal at maximum transmission, the output signal-to-noise ratio was 37.5 dB, and when the polarizer was rotated 45^{o} to simulate the crystal at minimum transmission the signal level fell by 30 dB. The limit to the maximum signal-to-noise ratio with either the crystal or the polarizer was the saturation current of the photodetector and therefore it can be concluded that the signal going through the crystal suffers a 7-dB loss of coherence for a narrowband signal. The crystal was mounted on an X-Y translation

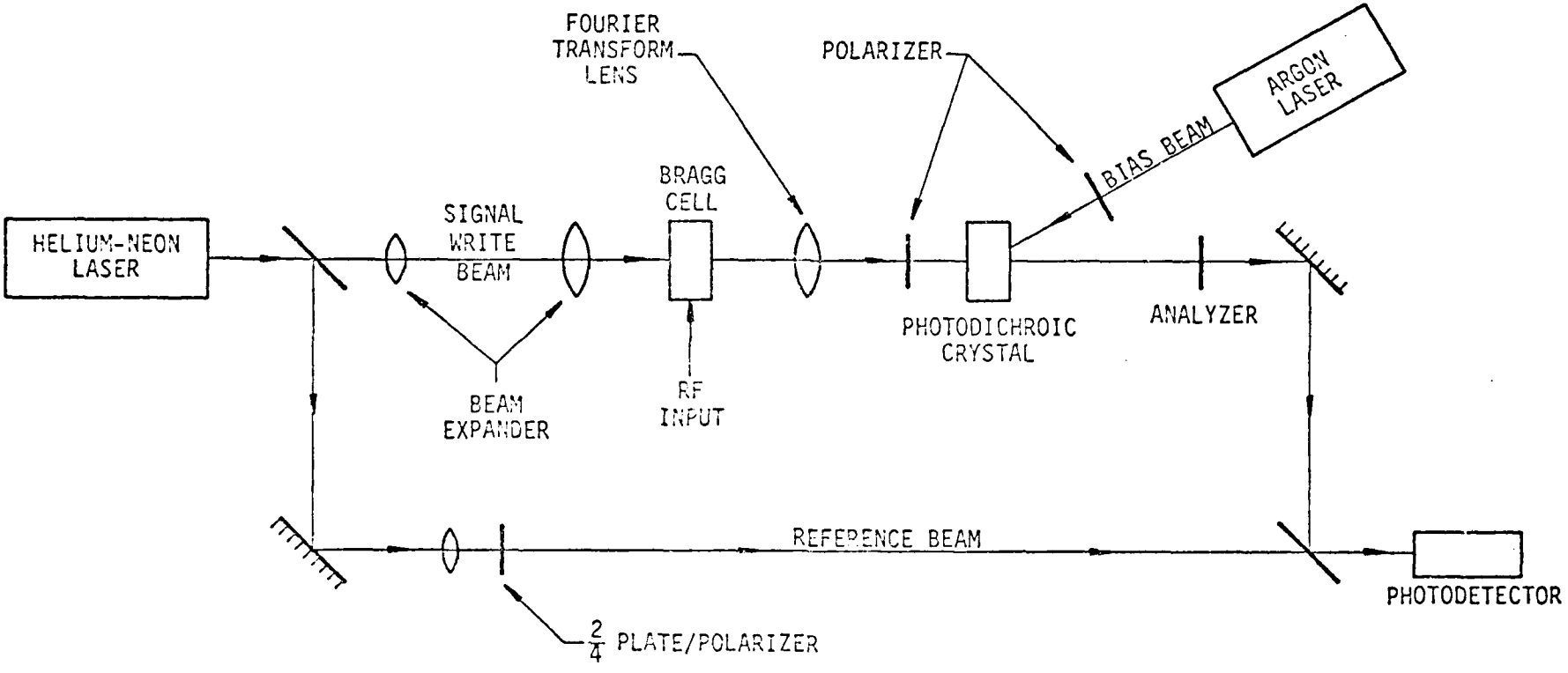

FIGURE 6-5

COHERENT SIGNAL PROCESSOR WITH OPTICAL CLIPPER AT TRANSFORM PLANE

6.2.2 Continued

stage and for each measurement the crystal was moved around until the maximum signal was obtained. In some regions of the crystals the signal loss was higher, sometimes as much as 10 dB more.

The other conclusion drawn from these measurements is that it would not be possible to use noise as a broadband input because at the output the injected noise would not exceed the output noise. With a noise-to-noise ratio of only 0 dB, the accuracy of the measurements would not be adequate to see the effect of the excisor on narrowband signals.

A noise-to-noise ratio of unity can be predicted by noting that the maximum signal-to-noise ratio for a narrowband signal was 30.5 dB in a 30-kHz noise bandwidth. If the noise bandwidth is expanded to the 40-MHz bandwidth of the optical excisor breadboard, the signal-to-noise ratio would drop by $40 \times 10^6 \div 30 \times 10^3$, or 31 dB. This would give a -0.5-dB signal-to-noise ratio for a narrowband signal and 40 MHz of noise, or likewise a noise-to-noise ratio of -0.5 dB in any analysis bandwidth. Without the 20-dB loss in the crystal the noise-to-noise ratio would be 19.5 dB and easily measured, but when the crystal was inserted into the processor the noise-to-noise ratio was negative.

The results of these narrowband signal measurements seemed encouraging because if ways could be found to reduce the insertion loss of the crystal then it should be possible to develop an optical excisor that could provide at least 23 dB of attenuation against a narrowband jammer. However, as explained in the following section, the insertion loss for a broadband signal was even higher. With the spread spectrum equipment at PROBE SYSTEMS it was possible to evaluate the photodichroic crystals in a coherent *and* broadband signal processor.

SECTION 7
SPREAD SPECTRUM MEASUREMENTS

Described in this section is a series of measurements using a spread spectrum signal generator as a signal source and a digital matched filter as a signal analyzer. This equipment at PROBE provided two significant benefits to the evaluation of the photodichroic crystals. First, the spread spectrum hardware provided a direct means to evaluate the coherence of a broadband signal that had passed through the photodichroic crystal. Second, the processing gain of the digital matched filter permitted accurate output signal-to-noise measurements even when the input signal level was below the noise.

7.1 TEST EQUIPMENT

The spread spectrum hardware was developed on an earlier program at PROBE to evaluate interceptor techniques. The heart of this equipment is a 200-MHz digital matched filter that was automatically loaded with the reference waveform that matched the spreading code used by the test signal generator. For the photodichroic evaluation the output of the test signal generator was centered at 70 MHz and chip rates could be varied from as low as 5 MHz up to a maximum of 50 MHz. Most of the measurements were made using a 20-MHz chip rate giving a null-to-null bandwidth of 40 MHz, thereby matching the 50- to 90-MHz passband of the optical excisor.

A block diagram of the spread spectrum electronics is shown in Figure 7-1. At the input, a signal from the spread spectrum test signal generator was summed with the output of a VHF oscillator which could be used to simulate an interfering narrowband signal. The sum of these signals was input to the excisor's electronic package. After filtering and amplification, the spread signal and interference provided the drive input to the Bragg cell in the optical processor.

Signals having been detected in the optical processor were amplified and filtered, then downconverted to baseband in the excisor's electronics package.

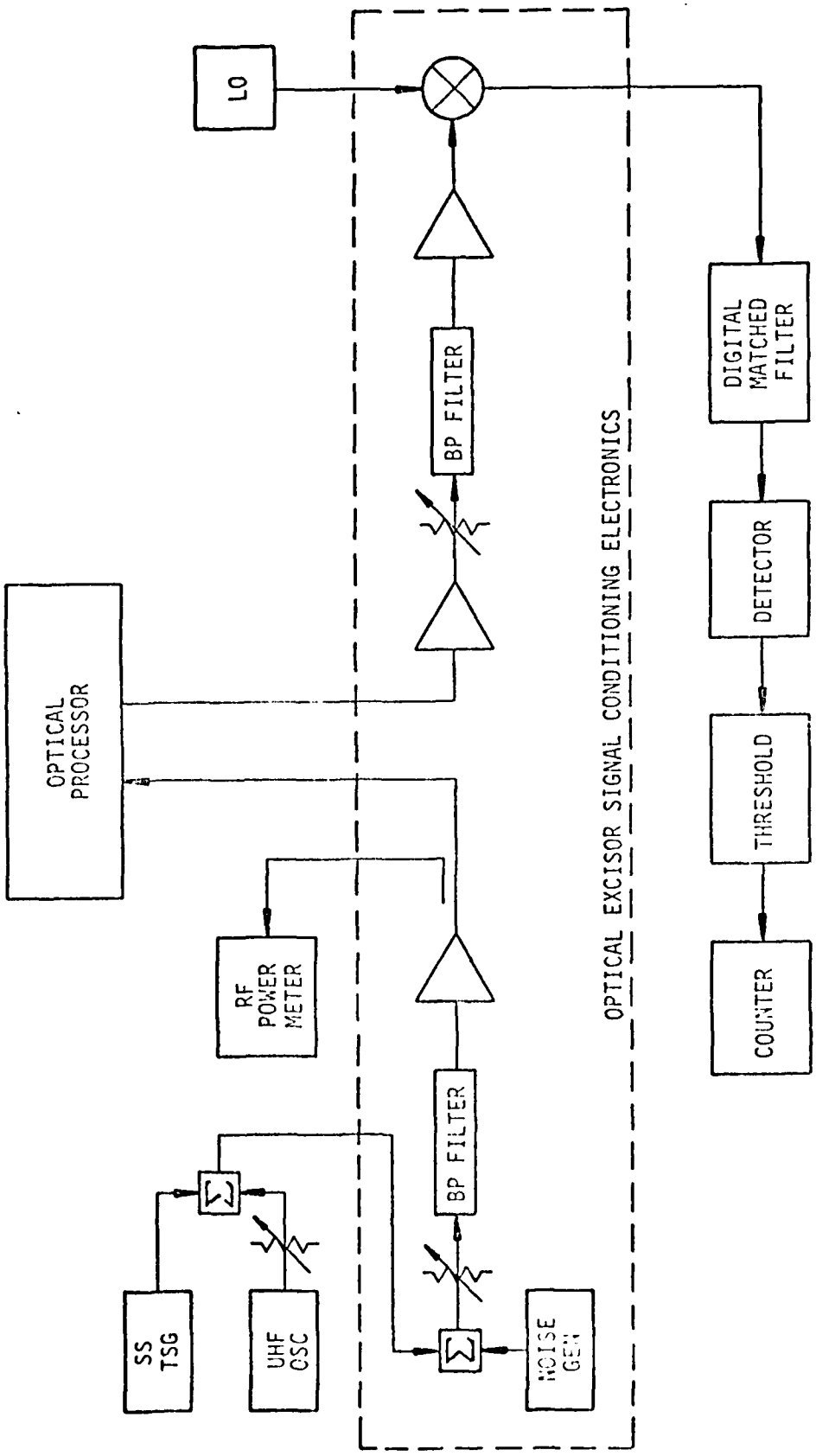

PSI-80056

FIGURE 7-1 ELECTRONIC SETUP FOR BROADBAND TEST

7.1 Continued

This downconverted output provided the input to the digital matched filter. Detection probabilities and false alarm rate are then measured at the filter output and are used to determine SNR at the output of the matched filter.

To estimate the excisor output signal-to-noise ratio, the processing gain of the matched filter must be subtracted from the filter's output signal-to-noise ratio. An analog matched filter with a time-bandwidth of 127 would give 21 dB of processing gain, but the 1-bit amplitude resolution of the digital matched filter would give a processing gain of no better than 19 dB. Laboratory measurements showed that the actual processing gain was 17 dB because of 2 dB implementation losses. When the test signal was sent through the optical excisor with the crystal removed before entering the matched filter, the processing gain was still 17 dB, indicating that the optical processor did not degrade the coherence of the spread signal or the signal-to-noise ratio. For example, if the detection-of-probability and false-alarm measurements indicate that the matched filter output signal-to-noise ratio was 10 dB, then by subtracting 17 dB it can be estimated that the excisor output signal-to-noise ratio (equal to the matched filter input signal-to-noise ratio) was -7 dB.

7.2 EXPERIMENTAL DATA

Optical excisor measurements with the spread spectrum signal were made first on the optical processor without a crystal. The spread spectrum test signal generator had a code repetition rate of 157.5 kHz, and after noise was added to this signal it was passed through the optical processor. The processor output then went through the digital matched filter, which gave an output pulse proportional to each correlation between the processor output and the reference code. When the input signal-to-noise ratio was 0 dB, the average number of detections per second was 145,000 when threshold was set for a 1.5×10^{-3} probability of false alarm, thereby giving a probability of detection of 92%. When the spread signal was lowered by 3 dB so that the input signal-to-noise ratio was -3 dB, the probability of detection fell to 64%, as expected.

7.2 Continued

When an interference signal was added such that the interference-to-noise ratio was 6 dB (and therefore the interference-to-signal ratio was 9 dB) the probability of detection fell to 4%. When a small wire was placed in the spectrum plane and positioned to block the narrowband interference, the probability of detection rose to 61%. The wire was such an effective excisor that the probability of detection did not change when the interference signal was removed, thereby proving that the signal loss from 64% down to 61% was due to the fraction of signal energy that was blocked by the wire as opposed to residual effects of an interference signal.

A series of measurements started when the crystal was installed in the optical excisor. The first measurements were with polarizers adjusted such that the crystal only had to behave like a window and was not required to rotate the polarization. The probability of detection fell to such low levels that the input noise source was removed and the spread spectrum signal level had to be increased before there was an output signal adequate for signal testing. This high insertion loss implied that the crystal severely affected the coherence of the light that was transmitted. Negative results were obtained from experiments to determine if the losses were due to lack of flatness or scattering, but visible strains and surface roughness seemed to indicate that both effects were destroying the coherence of the broadband signal.

The most encouraging results were obtained by using a UHF signal generator as an interference source set at a level 3.3 dB higher than the spread spread spectrum signal and then raising both signals until the 1-Watt limit on the Bragg cell level was reached. With the crystal used as an excisor (crossed polarizers), the number of detections per second was 251 compared to 400 detections per second when the interference was removed, and to 157 false alarms per second when both signals were removed.

When the crystal was used as a window (parallel polarizers), the spread spectrum signal had to be reduced by 16.6 dB to give a probability of

7.2 Continued

detection similar to the excisor configuration. At a false alarm rate of 160 per second, the number of detections per second fell from 525 down to 184 when the interference was added.

Therefore, it was possible to see some beneficial effects of the crystal because the crystal, when used as a window, gave 184 counts per second, but when used as an excisor the detection rose to 251 counts per second. Unfortunately, the losses in the crystal used up the breadboard model dynamic range to the point that higher interference levels could not be used, and hence more dramatic effects could not be measured accurately.

The unexpectedly low probability of detection was investigated by changing the bandwidth of the input signal and then changing the input signal level until the number of detections was approximately the same as the 500 detections per second achieved in the excisor experiments. The polarizers were rotated to be parallel and the crystal was not illuminated by the green bias light, and therefore the crystal was simply a window in these measurements.

By changing the chip rate in 1-MHz steps from 5 to 20 MHz, the insertion loss of the crystal was measured for sixteen different signal bandwidths. All the loss measurements were in the range of 8 to 10 dB, with the lower losses being at the lower bandwidths, thereby indicating that the light passing through the crystal was less coherent as the spot size increased. The 10-dB insertion loss when added to the 16.6-dB polarization loss (crossed vs. parallel polarizers), gave the crystal a total loss of 26.6 dB when used as an optical clipper in a broadband excisor.

SECTION 8
PHOTODICHROIC CONCLUSIONS

The measurements performed by PROBE SYSTEMS on the photodichroic crystals supplied by NRL proved the importance of evaluation a component as part of an actual system as opposed to an evaluation based on measuring the component characteristics. Specifically, the photodichroic crystals as supplied by NRL were found to meet or exceed the specifications of other crystals developed at NRL, but the crystals fell short of what is required of an optical clipper. The discrepancy between that was needed and what was supplied was not apparent until a spread spectrum signal was passed through the crystal. Coherent detection of this signal showed that passage through the crystal destroyed much of the coherence of the spread spectrum signal.

In retrospect, the disagreement between the forecasted performance of the crystals compared to the actual performance can be seen as the inability of the crystals to take on an optical quality suitable for interferometers. As stated in PROBE's proposal PSI-P-7162-01, Paragraph 3.1.3, the optical clipper should pass the desired signals and do so without distortion. If the optical clipper is not optically flat or has excessive scattering, it would then introduce phase and/or amplitude distortions to the output signal. The optical clipper must be a device suitable for use in a coherent optical processor and should have a one-way transmission that introduces less than one-quarter wavelength of phase distortion to the optical signal.

The crystals supplied to PROBE had an unusual lack of flatness and a high level of scattering. The exact causes of the poor optical quality could not be determined within the resources available for this task, but a combination of effects seemed to be responsible for the results. The lack of optical flatness could have been due to, in part, the cover glasses used to protect the crystals from water and water vapor. When the crystals were cooled, any difference in the coefficient of thermal expansion between the glass and the crystal or the cement used to bond the glass to the crystal could cause strains, and hence optical inhomogenities, in the crystal.

8. Continued

Another problem was caused by the crystals developing diffuser-like surfaces when held at a reduced temperature. It is not known if the degraded surfaces were caused by condensation of vacuum oil, but the lack of oil on the cold finger seemed to indicate that oil was only partially responsible for the diffuse surfaces. The diffuser effect was noticeable soon after the crystal was installed and the effect would get stronger with time until after a few days it became almost impossible to image any signal through the crystal.

Effects of optical scattering on laser beam quality by one of the photodichroic crystals is shown in Figure 8-1. Polaroid film was exposed directly by the laser beam in 8-1A at a distance of 2.2 m from the usual crystal location. Figure 8-1B was taken under the same conditions except that the crystal was in place. Scattering effects are evident.

Lack of flatness would degrade the coherence of the 40-MHz spread spectrum signal and the diffuser effect would degrade the detected signal strength even for narrowband signals. Crystal losses of 22 dB, even when the reference beam was combined with the signal beam before passing through the crystal, tends to prove that the diffuser effect was the principal loss mechanism. The final measurements on the last crystal which did not have cover glasses indicated that the crystal still had the ability to block narrowband interference power by more than 10 dB, but that the light transmitted was no longer sufficiently coherent to be useful in a real-time optical excisor.

In summary, the photodichroic crystals had appeared to be an ideal material for use in an optical excisor, but the measurements made in the PROBE SYSTEMS' breadboard model of an optical excisor show that a considerable amount of more work will be required to make the photodichroic crystals suitable for use in an optical processor using coherent detection of the light to generate a real-time RF output.

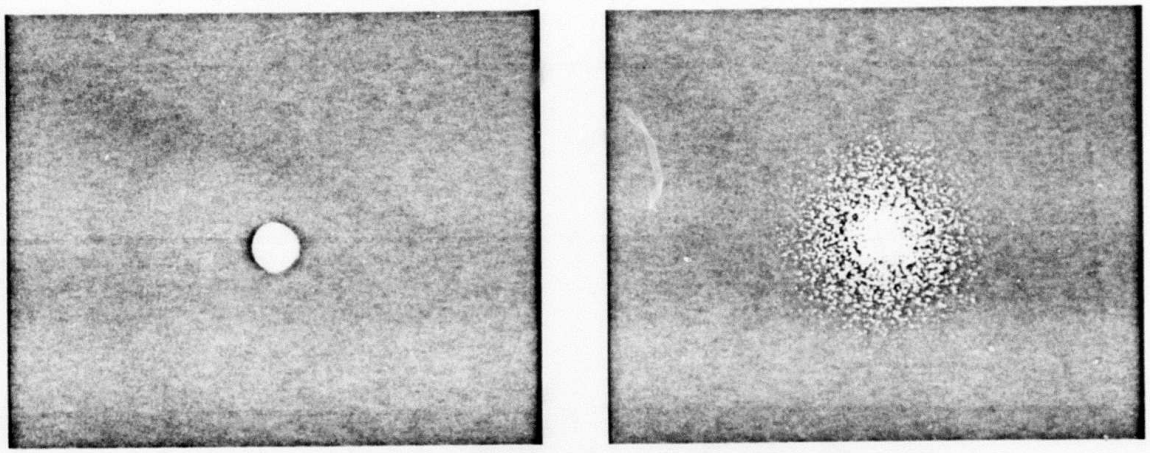

A. B.

FIGURE 8-1
OPTICAL SCATTERING BY THE PHOTODICHROIC CRYSTAL

SECTION 9
PHOTOCHROMIC GLASSES

Photochromic glasses were considered for use as optical clippers in the excisor. When activated, usually by long-wave UV or short-wave visible light, these glasses exhibit increased absorption across the visible spectrum. This change in transmission characteristics results from photo-ionization and re-combination of dopant ions and is a reversable process. Today, photochromic glass is most commonly used in self-darkening sunglasses.

In several respects, photochromic glass is an optimal material for use as a clipper -- long life, totally self-contained, no supporting electronics, etc. Its disadvantages are limited dynamic range and slow response time. To quantify the dynamic range and response time, PROBE evaluated a glass -- Corning Code 8111, "Photogrey Extra" -- in the lab. The sample was a plano-plano opthalmic lens blank.

Figure 9-1 shows the optical setup used to evaluate the sample. An argon laser operating at a wavelength of 488.0 nm was used to activate the sample and the transmission was monitored with a laser power meter. An aperture, 600 μm in diameter, limited the area of exposure and gave a spot of uniform illumination. This resulted in an incident optical power density of 71 mW/cm^2 on the glass sample.

Optical power was recorded as a function of time, providing the data plotted in Figure 9-2. In the response curve, we see a 3-dB change in attenuation in the first minute of exposure, which is approximately 4 J/cm^2. After 40 minutes the attenuation reached 5.5 dB.

The optical quality of the photochromic glass was outstanding, and therefore only the contrast and the relatively slow response time limit the utility of photochromic glasses as optical clippers. Recent advances in new photochromic glass may provide additional contrast and hence a deeper excision

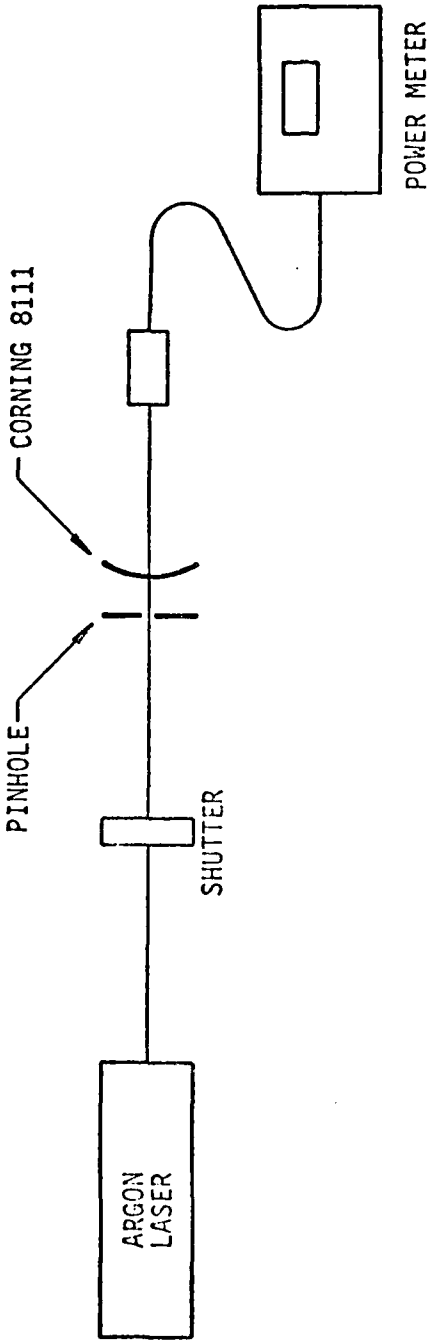

FIGURE 9-1 PHOTOCHROMIC GLASS TEST SETUP

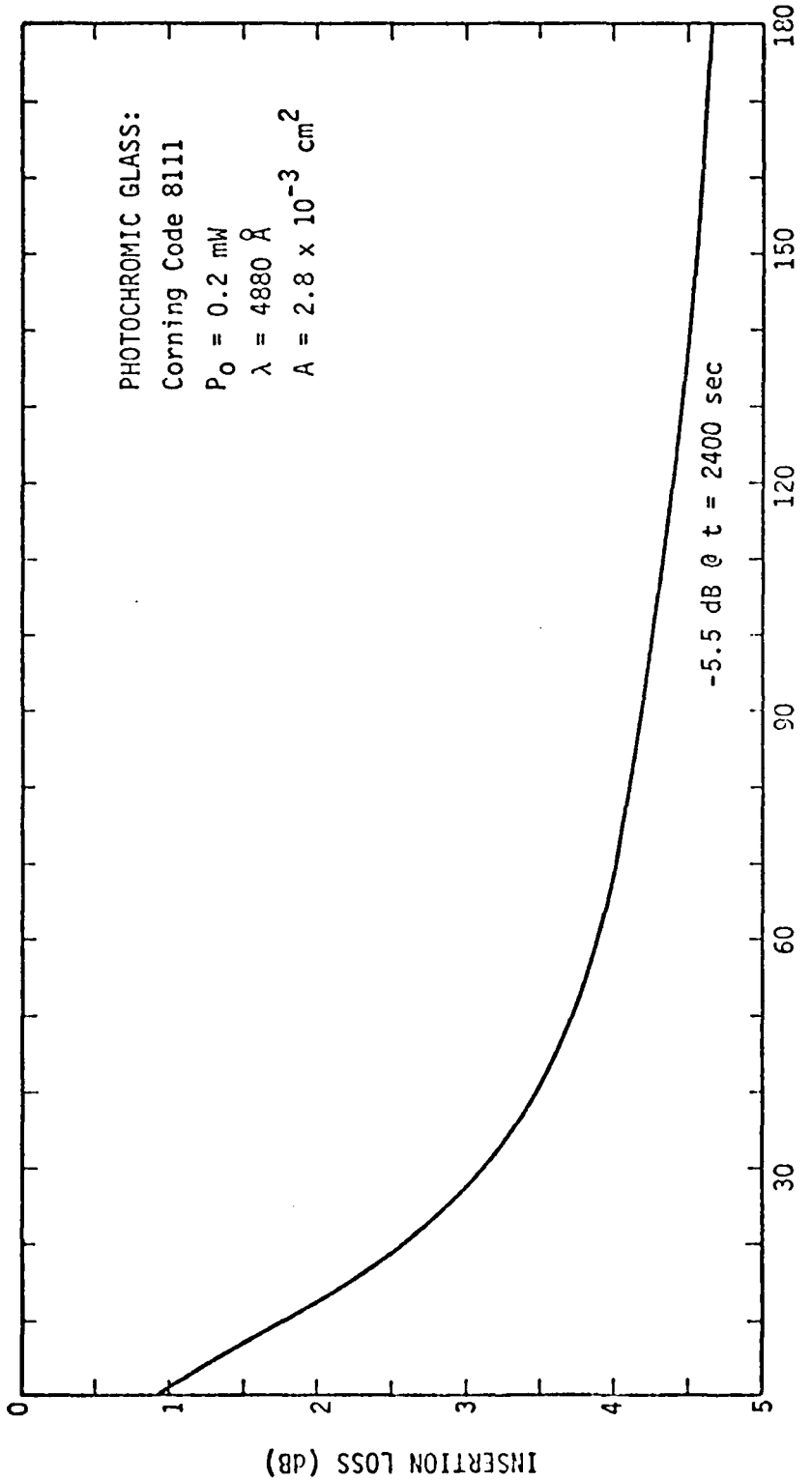

FIGURE 9-2 ATTENUATION AS A FUNCTION OF TIME FOR PHOTOCHROMIC GLASS

PSI-80094

9. Continued

notch, and they may also have a shorter response time. Until new glasses are released, an optical excisor using photochromic glass will be useful primarily for those applications where the interference levels only need to be reduced less than 10 dB and where the frequency of each interference signal is only slowly changing.

SECTION 10
OPTICAL CLIPPER CONCLUSIONS

The work reported here evaluated optical clipper materials that have the potential to minimize the effects of narrowband RF interference when used in a unique optical processor. The most successful results were obtained with the PROM, an optically addressed optical memory. In the optical excisor the PROM was able to attenuate the interference by nearly three orders of magnitude. Another material evaluated was photodichroic crystals, but the optical quality and scattering significantly reduced the utility of this type of optical clipper. A photochromic glass was found to provide only 5 dB of attenuation, but it was by far the easiest optical clipper to use.

Further development of optical clippers is recommended because the laboratory results clearly demonstrate the ability of an optical excisor to provide orders of magnitude improvements in broadband RF receiver performance. However, optical clipper improvements are needed before a practical optical excisor can be developed using an optical clipper. At this time, a more practical approach is to replace the optical clipper with the electronic clipper described in PROBE SYSTEMS' Report No. PSI-ER-5538-02.